MOLECULAR AND CELLULAR BIOLOGY, July 2005, p. 6047–6064 Vol. 25, No. 14
0270-7306/05/$08.00+0 doi:10.1128/MCB.25.14.6047–6064.2005

Activation of a Nuclear Cdc2-Related Kinase within a Mitogen-Activated Protein Kinase-Like TDY Motif by Autophosphorylation and Cyclin-Dependent Protein Kinase-Activating Kinase

Zheng Fu,[1] Melanie J. Schroeder,[2] Jeffrey Shabanowitz,[2] Philipp Kaldis,[3] Kasumi Togawa,[4] Anil K. Rustgi,[4] Donald F. Hunt,[2,5] and Thomas W. Sturgill[1]*

Departments of Pharmacology and Internal Medicine,[1] Chemistry,[2] and Pathology,[5] University of Virginia, Charlottesville, Virginia, 22908; Mouse Cancer Genetics Program, National Cancer Institute, Frederick, Maryland 21702[3]; and Division of Gastroenterology, Departments of Medicine and Genetics, Cancer Center, University of Pennsylvania, Philadelphia, Pennsylvania 19104[4]

Received 13 December 2004/Returned for modification 21 January 2005/Accepted 4 April 2005

Male germ cell-associated kinase (MAK) and intestinal cell kinase (ICK) are nuclear Cdc2-related kinases with nearly identical N-terminal catalytic domains and more divergent C-terminal noncatalytic domains. The catalytic domain is also related to mitogen-activated protein kinases (MAPKs) and contains a corresponding TDY motif. Nuclear localization of ICK requires subdomain XI and interactions of the conserved Arg-272, but not kinase activity or, surprisingly, any of the noncatalytic domain. Further, nuclear localization of ICK is required for its activation. ICK is activated by dual phosphorylation of the TDY motif. Phosphorylation of Tyr-159 in the TDY motif requires ICK autokinase activity but confers only basal kinase activity. Full activation requires additional phosphorylation of Thr-157 in the TDY motif. Coexpression of ICK with constitutively active MEK1 or MEK5 fails to increase ICK phosphorylation or activity, suggesting that MEKs are not involved. ICK and MAK are related to Ime2p in budding yeast, and cyclin-dependent protein kinase-activating kinase Cak1p has been placed genetically upstream of Ime2p. Recombinant Cak1p phosphorylates Thr-157 in the TDY motif of recombinant ICK and activates its activity in vitro. Coexpression of ICK with wild-type CAK1 but not kinase-inactive CAK1 in cells also increases ICK phosphorylation and activity. Our studies establish ICK as the prototype for a new group of MAPK-like kinases requiring dual phosphorylation at TDY motifs.

Mitogen-activated protein kinases (MAPKs) are defined by characteristic regulation by dual tyrosine and threonine phosphorylation in a TXY motif in the T loop (27). The major cell cycle transitions are governed by spatial and temporal activity of cyclin-dependent protein kinases (CDKs) (26). Active CDK/cyclin heterodimers require T-loop phosphorylation at a threonine site in CDKs that aligns with the regulatory threonine site of MAPKs (7). MAPKs are regulators in the cell cycle. For example, extracellular signal-regulated kinase 2 (ERK2) regulates cyclin D1 transcription and destabilizes $p27^{Kip}$ (29) to promote entry into the cell cycle. To halt the cell cycle, p38 MAPK α/β inhibits cyclin D1 transcription (21) and destabilizes cyclin D1 (8).

Products of human genes CDKL1, CDKL2, CDKL3, ICK, MAK, and MOK have similarity to both CDKs and MAPKs. All except MOK have a TDY motif in the T loop that aligns to the TXY motif of classic MAPKs such as ERK2 (see Fig. 1B). CDKL1, CDKL2, and CDKL3 cluster together in similarity. Male-germ cell associated kinase (MAK) (20) and intestinal cell kinase (ICK) (40) are closely related to each other. MOK has a TEY motif but is most similar to MAK and ICK. MAK, ICK, and MOK each associates with human Cdc37 and Hsp90 (25).

ICK was cloned from a crypt cDNA library by using a degenerate PCR strategy for MAPKs (40). The intestinal crypt is the compartment of the intestinal epithelium where proliferation and specification of different lineages occur (30). Expression of ICK mRNA in intestinal epithelium was localized specifically to the crypt compartment by in situ staining (40).

Available data from public serial analysis of gene expression and microarrays suggest that ICK mRNA may be ubiquitously expressed in human tissues. Northern analyses with a specific 3′ probe to human ICK detected an ~6 kb mRNA in most tissues examined (40, 44). MAK expression is restricted in comparison. MAK mRNAs (3.8 and 2.6 kb) are expressed in male germ cells at and after meiosis in testis (23). However, MAK expression is not restricted to testis. MAK is expressed in normal retina (6) and was identified as an androgen-inducible gene in LNCaP prostate epithelial cells (42). Like MAK, ICK has specific patterns of temporal and spatial expression in embryos and adult tissues (4, 40). Functions are yet to be defined and could possibly be overlapping in tissues such as testis where both are expressed. A $MAK^{-/-}$ mouse is viable and fertile (37).

Here, we establish ICK as the prototype for a new group of kinases with MAPK-like regulation at TDY motifs. ICK (40) and MAK (42) require an intact TDY motif for activity. We

* Corresponding author. Mailing address: Department of Pharmacology, University of Virginia School of Medicine, 1300 Jefferson Park Avenue, Charlottesville, VA 22908-0735. Phone: (434) 924-9191. Fax: (434) 924-5207. E-mail: Thomas_Sturgill@virginia.edu.

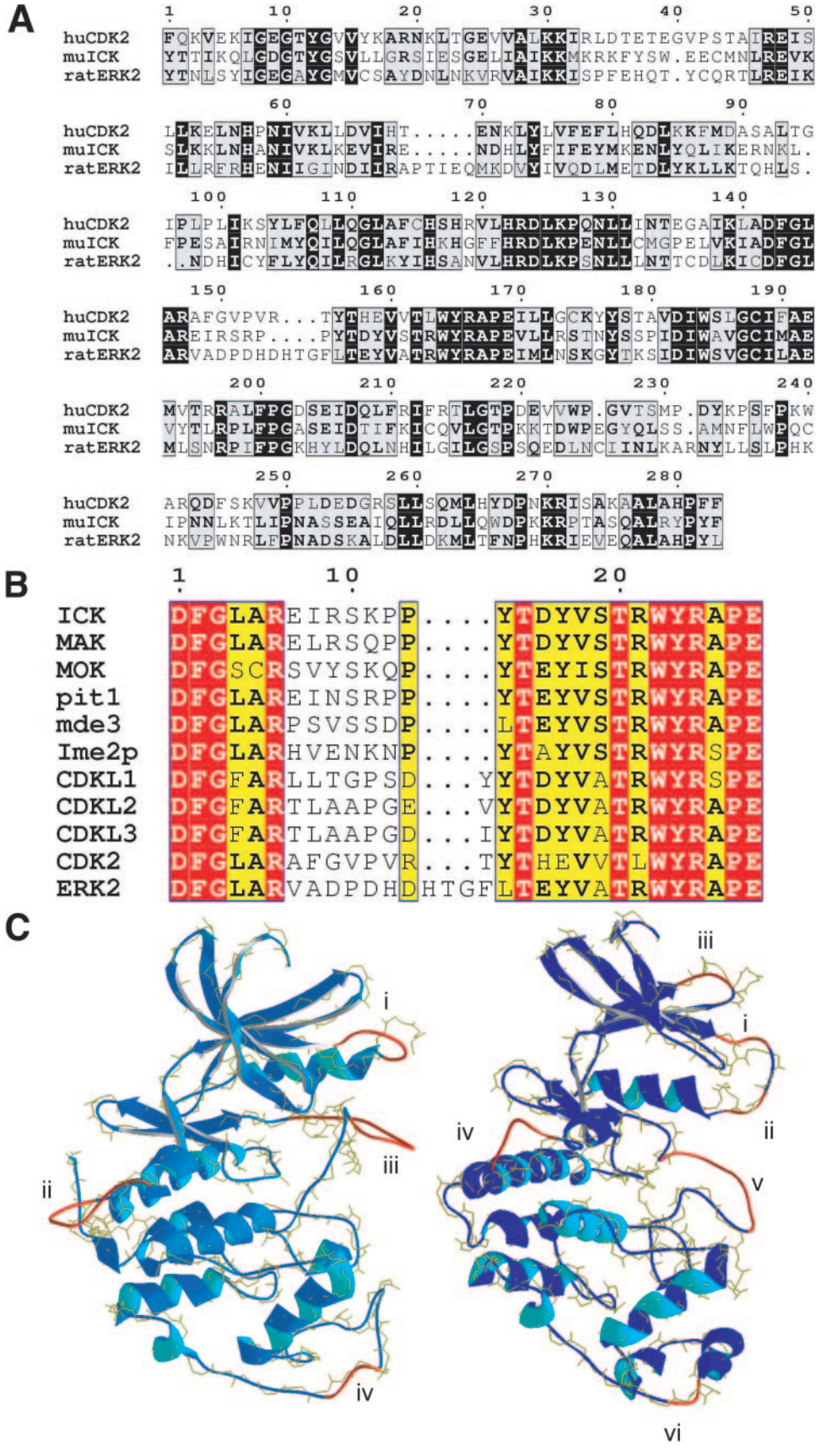
A
huCDK2
muICK
ratERK2
B
ICK
MAK
MOK
pit1
mde3
Ime2p
CDKL1
CDKL2
CDKL3
CDK2
ERK2
C
i
ii
iii
iv
v
vi

show that the TDY motif of ICK is phosphorylated in cells and dual phosphorylation is required for maximum activity. Activation of ICK requires autokinase activity and CDK-activating kinase (CAK) phosphorylation. We define structural requirements for nuclear localization and independence of localization from activity and demonstrate a requirement for nuclear localization for dual phosphorylation and activation. Thus, ICK is a Cdc2-related nuclear kinase regulated similarly to classic MAPKs and may modify nuclear events in proliferation and development.

MATERIALS AND METHODS

Plasmid construction. Mouse ICK sequences of wild type (WT), KD (K33R), ADF, ADY, and TDF were cloned into pEBG-GST as described previously (40). An IMAGE clone (MGC 46090) of the human ICKb sequence was purchased from IMAGE Consortium. pCDNA3-Flag-NES was kindly provided by Bryce Paschal and constructed by Adam Spencer (Center for Cell Signaling, University of Virginia). Two annealed DNA oligonucleotides that encode the nuclear export sequence (NES) (NELALKLAGLDINK) of the protein kinase inhibitor of protein kinase A were synthesized with a 5′-HindIII overhang and a 3′-BamHI overhang and cloned into pCDNA3-Flag (Invitrogen). pCDNA3-Flag-hBMK1 and pCMV-HA-rMEK5(DD) were generous gifts from Bradford C. Berk (University of Rochester). pCMV-HA-rMEK1(DD) was kindly provided by Michael J. Weber (University of Virginia). CAK1wt and CAK1(N161A) were PCR amplified from yeast expression constructs (15) and subcloned into mammalian expression vector pCDNA3.1 by Aiyang Cheng (Mark Solomon, Yale University). To generate pEBG-GST-rERK2, rat ERK2 sequence was PCR amplified and cloned into the pEBG-GST vector at the 5′-SpeI and 3′-NotI sites.

Mouse ICK sequences of WT, KD, and ADF and human ICKb sequence were amplified using primers incorporating a 5′-BglII site and a 3′-EcoRI site and cloned into pEGFP-C3 (Clontech). The ICKb sequence was amplified using primers incorporating a 5′-SpeI site and a 3′-NotI site and cloned into pEBG-GST. C-terminally truncated sequences of ICK were generated by PCR and cloned into pEBG-GST and pEGFP-C3. The point mutations K270A, K271A, R272A, K270A/K271A, K270A/K271A/R272A, E169A, W184A in the full-length mouse ICK sequence were generated by using a four-primer PCR method and cloned into pEBG-GST and pEGFP-C3. All mutations were confirmed by sequencing. The full-length mouse ICK sequence, a subset of C-terminal truncation sequences (positions 1 to 277, 1 to 284, 1 to 291, and 1 to 300), and ADF, ADY, and TDF mutants of mouse ICK(1 to 300) were PCR amplified and cloned into pGEX4T-1 at the 5′-EcoRI and 3′-NotI sites.

To construct pEGFP-C3-Flag-NES-mICK, the mouse ICK sequence was amplified and cloned into pCDNA3-Flag-NES at the 5′-NotI and 3′-XbaI sites to generate pCDNA3-Flag-NES-mICK. The sequence encoding Flag-NES-mICK was then amplified and cloned into pEGFP-C3 at the 5′-BglII and 3′-EcoRI sites.

Cell culture and transient transfection. HEK293T and COS-7 cells were maintained at 37°C and 5% CO_2 in Dulbecco's modified Eagle's medium supplemented with 10% fetal bovine serum. At 60 to 80% confluence, COS-7 cells were transfected using Lipofectamine 2000 (Invitrogen). At 30 to 40% confluence, HEK293T cells were transfected using a calcium phosphate protocol.

Immunofluorescence. COS-7 cells were grown on coverslips in six-well dishes. Cells were continually grown for 7 to 8 h after transfection, rinsed briefly in phosphate-buffered saline (PBS), and fixed in 4% formaldehyde in PBS for 20 min at room temperature (RT), followed by extensive rinses in PBS. Coverslips were mounted using Vectashield mounting medium containing DAPI (4′,6′-diamidino-2-phenylindole). Cells were observed under a Zeiss Axiovert microscope equipped with a Hammatsu Orca camera. Images were processed using Openlab software.

GST pull-down. HEK293T cells were transfected with 5 to 10 μg of glutathione *S*-transferase (GST)-ICK plasmid for 7 to 8 h and were continually grown in fresh Dulbecco's modified Eagle's medium with 10% fetal bovine serum for another 24 to 36 h. Cells were harvested in ice-cold PBS, and lysed in lysis buffer (50 mM Tris-HCl, pH 7.4, 150 mM NaCl, 1% NP-40, 2 mM EGTA, and 2 mM dithiothreitol [DTT] supplemented with complete protease inhibitors [Roche], 1 mM Na_3VO_4, 1 μM microcystin LR, and 5 mM β-glycerophosphate). The cell lysate was cleared by centrifugation. The GST-ICK fusion proteins were absorbed on glutathione-Sepharose beads. The beads were washed extensively with lysis buffer followed by kinase buffer (50 mM HEPES, pH 7.5, and 10 mM $MgCl_2$ supplemented with 5 mM DTT, protease inhibitors, and phosphatase inhibitors).

In vitro kinase assay and Cak1p phosphorylation. The GST pull-down samples were incubated with 5 μCi [γ-^{32}P]ATP (7,000 Ci/mmol), 100 μM ATP, and 5 μg myelin basic protein (MBP) in 50 μl kinase buffer at 30°C for 15 min. The reaction was terminated by addition of 50 μl 2× sodium dodecyl sulfate (SDS) sample buffer. The reaction sample was heated for 5 min and separated on a 12% SDS gel. The gel was dried and exposed for autoradiograph and PhosphorImager analyses. For Cak1p phosphorylation, GST-ICK(1–300) (1 to 2 μg) or GST-CDK2 (2 μg) was incubated with GST-Cak1p (20 ng) in the presence of 5 μCi [γ-^{32}P]ATP (7,000 Ci/mmol) and 20 μM ATP at RT for 30 min. The preparation of GST-Cak1p and GST-CDK2 was described previously (18).

Phosphatase treatment. The GST pull-down samples were washed in lysis buffer followed by HEPES buffer (50 mM HEPES, pH 7.5, and 10 mM $MgCl_2$, supplemented with 5 mM DTT, protease inhibitors, and 2 mM $MnCl_2$ for protein phosphatase 2A (PP2A) and lambda protein phosphatase treatment or 1 mg/ml bovine serum albumin for *Yersinia* protein tyrosine phosphatase treatment). The beads were incubated with either 10 units of calf intestine phosphatase (New England BioLabs), 0.5 unit of purified PP2A (a gift of David Brautigan, University of Virginia), 50 units of lambda protein phosphatase (New England BioLabs), or 50 units of *Yersinia* protein tyrosine phosphatase (New England BioLabs) at 30°C for 15 to 45 min with gentle agitation. The beads were washed extensively with kinase buffer supplemented with phosphatase inhibitors and subjected to the kinase reaction. For PP2A inhibition, 1 μM okadaic acid (Calbiochem) was used in the reaction.

Western blotting. The SDS sample was separated on a 10% SDS gel and transferred. The polyvinylidene difluoride membrane was blocked overnight at 4°C with 5% dry milk in PBS-Tween 20, probed with primary antibodies (1.0 μg/ml anti-phosphoERK [Promega], 0.2 μg/ml anti-GST [B-14] [Santa Cruz], 0.1 μg/ml anti-Flag M2 [Sigma], 0.1 μg/ml antihemagglutinin [anti-HA] [Sigma], 1.0 μg/ml antiphosphotyrosine [clone 4G10] [Upstate], and 0.1 μg/ml anti-ICK) for 1 to 2 h at RT followed by horseradish peroxidase-conjugated secondary antibodies (1:10,000 dilution; Pierce) for 1 h at RT. The immunoblot was visualized using an ECL detection system (Amersham).

GFP-ICK immunoprecipitation. Green fluorescent protein (GFP)-ICK constructs were transfected into HEK293T cells grown in 10-cm dishes. Cells were harvested and lysed in lysis buffer supplemented with protease and phosphatase inhibitors. The cell lysate obtained from one 10-cm dish was incubated with 1 to 2 μg of monoclonal anti-GFP antibody (Roche) at 4°C for 2 to 3 h. The immune complex from the cell lysate was pulled down by incubation with 30 μl protein A-agarose beads at 4°C for 1 to 2 h. The beads were washed extensively with lysis buffer followed by kinase buffer for assay.

In vivo MEK phosphorylation. GST-ICK was cotransfected with either HA-MEK1(DD) or HA-MEK5(DD) into HEK293T cells. As controls, GST-ERK2 was cotransfected with HA-MEK1(DD) and Flag-ERK5 with HA-MEK5(DD). The cell lysate was incubated with either glutathione-Sepharose beads to pull down GST-ICK and GST-ERK2 or 0.5 to 1.0 μg anti-Flag M2 monoclonal antibody (Sigma) plus protein A-agarose beads to pull down Flag-ERK5. Beads were extensively washed with lysis buffer followed by kinase buffer. Equal ali-

FIG. 1. ICK is a MAPK- and CDK-like kinase with a TDY motif. (A) Sequence alignment of the catalytic domains of mouse ICK, rat ERK2, and human CDK2 by using Clustal. ICK shares about 38% to 40% overall identity to ERK2 and CDK2 in the catalytic domains shown. ICK, MAK, and MOK have short N termini like CDK2, each only three residues (not shown). ICK also contains a C-terminal domain (not shown) that is similar to that of MAK but more divergent. Numbering corresponds to the catalytic domain residues. (B) Alignment of the T loops of TDY motif kinases in the human genome. Ime2p, pit1, and mde3 are putative homologs of ICK and MAK in yeast. (C) SwissModel models of ICK(1–291) to CDK2 (left) and to ERK2 (right). ICK is shown in each model as a ribbon, with segments having high B factors (35) versus the template in red (see text for details). The backbone of the template with its oxygens is shown in yellow for comparison. The calculated final total energies for the models to CDK2 and ERK2 were −9,910 and −10,700 kJ/mol, respectively.

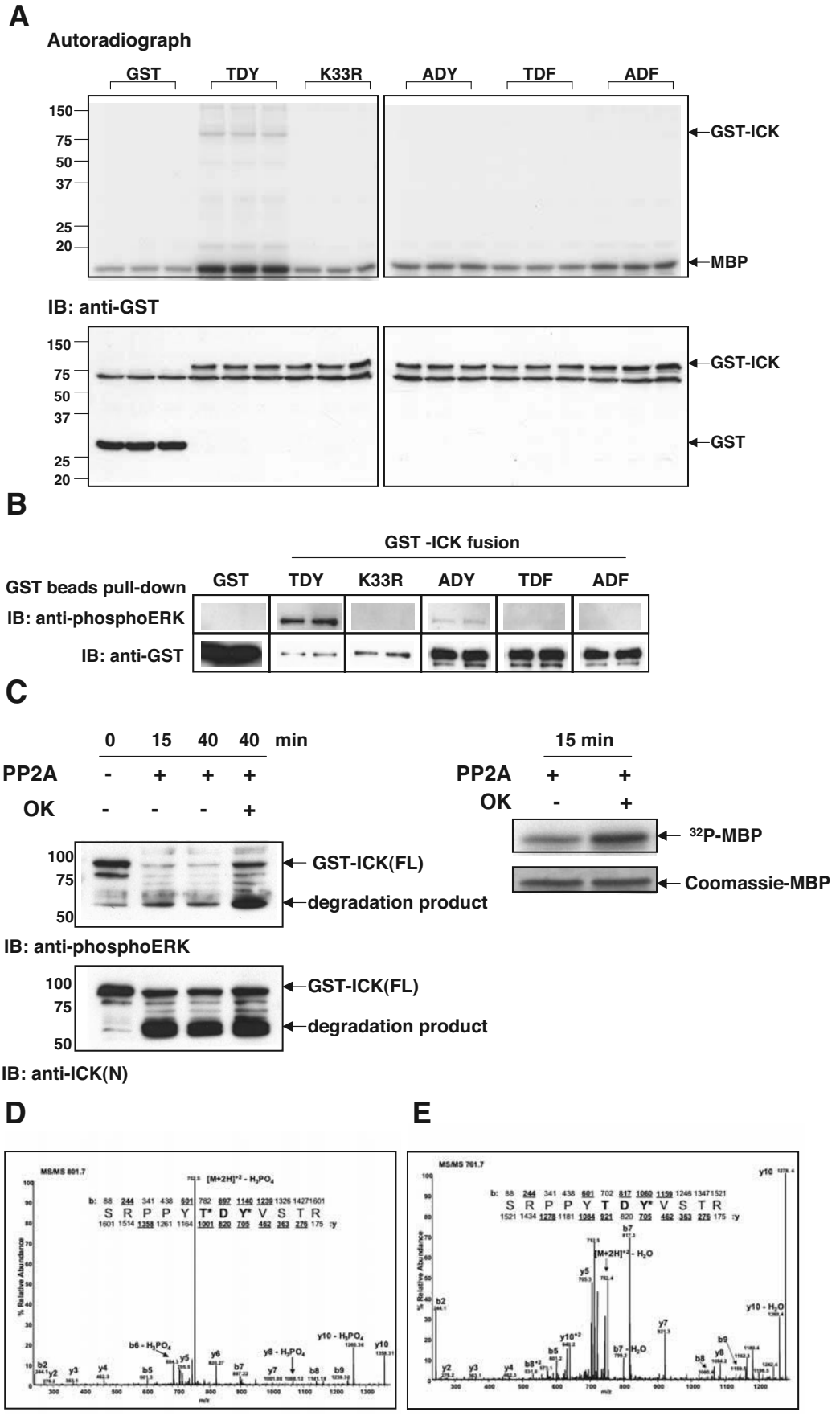
A
Autoradiograph
GST
TDY
K33R
ADY
TDF
ADF
150
75
50
37
25
20
GST-ICK
MBP
IB: anti-GST
GST-ICK
GST
B
GST -ICK fusion
GST beads pull-down
GST
TDY
K33R
ADY
TDF
ADF
IB: anti-phosphoERK
IB: anti-GST
C
0 15 40 40 min
PP2A - + + +
OK - - - +
100
75
50
GST-ICK(FL)
degradation product
IB: anti-phosphoERK
GST-ICK(FL)
degradation product
IB: anti-ICK(N)
15 min
PP2A + +
OK - +
32P-MBP
Coomassie-MBP
D
E

quots of bead sample were subjected to either in vitro kinase assay or immunoblot analysis.

In vivo CAK1 phosphorylation. GST-ICK, GST-ICK(1–300), or GST-ERK2 was cotransfected with either CAK1(WT) or CAK1(N161A) mutant in HEK293T cells. The cell lysate was incubated with glutathione-Sepharose beads to pull down GST fusion proteins. Beads were extensively washed with lysis buffer followed by kinase buffer and subjected to either immunoblot analysis or in vitro kinase assay. The expression of CAK1(WT) and CAK1(N161A) mutant in the cell lysate was analyzed with anti-CAK1 monoclonal antibody (15).

Production of GST-ICK fusion in *Escherichia coli*. Plasmids expressing full-length or C-terminally truncated mouse ICK sequences were transformed into TOP-10 (Invitrogen). Bacteria were grown up at 37°C and 200 rpm until the optical density at 600 nm reached 0.6 to 0.8. Protein expression was induced with 0.2 mM IPTG (isopropyl-β-D-thiogalactopyranoside) at 37°C and 200 rpm for 1 to 2 h. Bacteria were harvested by centrifugation and lysed in 1× PBS buffer (pH 7.4) containing 2 mM EDTA, 2 mM DTT, protease inhibitors, phosphatase inhibitors, and 0.1 mg/ml lysozyme. After pulse sonication, the bacterial lysate was clarified by centrifugation and then incubated with glutathione-Sepharose beads at 4°C for 2 h. Beads were washed extensively with lysis buffer followed by kinase buffer before being subjected to in vitro kinase assay and immunoblot analysis.

ICK antibody. A C-terminal peptide, [C]RIDWSSKYPSRR (residues 618 to 629 of mouse ICK), and a N-terminal peptide, [C]MNLREVKSLKK (residues 46 to 56 of mouse ICK), were coupled to keyhole limpet hemocyanin. The rabbit antiserum was purified on a peptide affinity column (Sulfolink; Pierce). The eluted antibody was dialyzed against PBS, concentrated, and stored frozen in 50% glycerol. These two ICK antibodies were referred to as anti-ICK(C) and anti-ICK(N), respectively.

Molecular modeling. Modeling of mouse ICK used programs on the server at the Swiss Institute of Bioinformatics. SwissModel chose five CDK2 templates in automated mode (1h07, 1okvc, 1buh, 1hck, and 1pxj). ICK was modeled separately to unphosphorylated rat ERK2 (1erk). Analyses and images were made using DeepView on a G4 Macintosh computer. Only the trace for 1hck was used in the rendered image for the ICK to CDK2 model.

Mass spectrometry. Affinity-purified GST-ICK from HEK293T cells was separated by SDS-polyacrylamide gel electrophoresis, and the Coomassie blue-stained band was excised for in-gel digestion with trypsin (technique modified from that described in reference 36). Extracted peptides were separated by nanoflow high-pressure liquid chromatography (33) and analyzed online with an LCQ Deca XP ion trap mass spectrometer (Thermo Electron, San Jose, CA). A targeted method was used in which the *m*/*z* values for the +2 and +3 charge states of the tryptic peptide, SRPPYTDYVSTR, in the nonphosphorylated and singly phosphorylated forms and the +2 charge state of the doubly phosphorylated form were exclusively subjected to tandem mass spectrometry (MS/MS) (collision energy set to 35%, precursor mass ± 1.5 Da). For comparison of GST-ICK(1–300) from *E. coli* and HEK293T cells, the GST-ICK(1–300) bound to glutathione beads was subjected to on-bead digestion (10). ICK on beads was reduced with DTT and alkylated with iodoacetamide. Enzymatic digestion was achieved with overnight trypsin digestion (500 ng; Promega) at RT. An aliquot corresponding to 10% of the acidified digest was analyzed as described above except that the +2 charge states of the nonphosphorylated and doubly phosphorylated forms were targeted along with the +2 and +3 charge states of the singly phosphorylated form. The gradient (33) was shortened to 0 to 60% B in 40 min. The tyrosine phosphopeptide SRPPYTDY*VSTR was synthesized with standard solid-phase 9-fluorenylmethoxy carbonyl chemistry for comparison of MS/MS fragmentation patterns (data not shown).

RESULTS

Modeling of ICK to CDK2 and ERK2. The catalytic domains of ICK, CDK2, and ERK2 are 38 to 40% identical in ~280 residues of overlapping sequence (Fig. 1A). The catalytic domain of ICK(4–284) has more similarity overall to CDK2 than to ERK2. The Smith-Waterman score for alignment of the catalytic domains of murine ICK and human CDK2 is 720 (3.3 E-47). By comparison, the score for ICK alignment to rat ERK2 is 626 (9.4 E-41). The T loops of ICK, CDK2, and ERK2 are compared to the other TDY motif kinases in Fig. 1B. The activation loops of ICK, MAK, and MOK are one residue shorter than that of CDK2 and four residues shorter than that of ERK2.

To obtain further insights into the putative ICK structure, we used SwissModel (35). SwissModel generated a model for ICK(1–290) with the ICK and CDK2 backbones nearly superimposed (Fig. 1C, left). SwissModel calculates B factors (not equivalent to the familiar crystallographic factors; see SwissModel online) whose magnitudes inversely correlate with fit. The highest B factors were at (i) residues 35 to 43 between the predicted β1 strand and α_c helix, (ii) residues 92 to 100 between predicted α_e and α_d helices, (iii) residues 146 to 155 in the T loop, and (iv) residues 236 to 239 in the loop separating subdomain X and subdomain XI. The threonine residue in the TDY motif was 4.82 Å (root mean square deviation [RMSD], residue atoms) from the threonine residue in the THE motif in CDK2 phosphorylated by CAK. The most similar segment of the T loops (ICK residues 157 to 172) was within 0.31 Å (RMSD, backbone atoms) of the corresponding segment in CDK2.

In some segments, ICK is more similar to ERK2 than to CDK2. For example, residues from the TDY motif to the APE motif in the T loop are more similar to ERK2 (Fig. 1A). When ERK2 was used as the template, the backbones of predicted ICK(1–290) and ERK2 were nearly superimposable except in five short segments (Fig. 1C, right). The highest B factors for this ICK model were at (i) residues 36 to 39 and 42 to 43 between the predicted β_1 strand and α_c helix, (ii) residues 70 to 72 between β_4 and β_5 where ERK2 has an insertion that is not present in ICK and CDK2, (iii) residues 93 to 97, (iv) residues 148 to 157 in the T loop, and (v) residues 237 to 239.

In ICK modeled to inactive ERK2, the tyrosine residue of the TXY motif was buried as in ERK2 and superimposed within 0.06 Å (RMSD, all residue atoms). The backbone atoms of the aspartate residue in the TDY motif were within 0.03 Å

FIG. 2. The TDY motif of ICK is dually phosphorylated in cells, and phosphorylation is required for ICK activity. (A) In vitro kinase assay using GST-ICK and mutants. GST fusion proteins expressed in HEK293T cells were partially purified on glutathione-Sepharose beads. The bead samples were subjected to kinase assay using MBP as the substrate (top panel). The expression of GST fusions was assayed with anti-GST antibody (bottom panel). IB, immunoblotting. (B) Immunoreactivities of GST-ICK and mutants against the anti-phosphoERK antibody. The bead samples were prepared essentially as described for panel A. Equal portions of beads were blotted against anti-phosphoERK and anti-GST antibodies, respectively. (C) Dephosphorylation of GST-ICK by PP2A. GST-ICK was treated with PP2A in the absence or presence of 1 μM okadaic acid (OK) and either blotted against anti-phosphoERK and anti-ICK(N) antibodies (left panel) or subjected to in vitro kinase assay using myelin basic protein (right panel). Note that a major degradation product of about 60 to 65 kDa was enriched after PP2A treatment. This lower band was recognized by both anti-phosphoERK and anti-ICK(N) antibodies. (D) Tandem mass spectrum of the TDY tryptic peptide, showing dual phosphorylation of the TDY motif in ICK. (E) Tandem mass spectrum of the singly phosphorylated TDY peptide from ICK. Abundant, unlabeled peaks are accounted for in the corresponding MS/MS spectrum of the synthetic tyrosine-phosphorylated peptide (data not shown).

(RMSD) of the corresponding glutamate residue in the TEY motif in ERK2. The threonine residue in the TDY motif was more distant, 5.04 Å (RMSD), from the corresponding threonine residue in the ERK2 TEY motif. The backbone atoms in the most similar portion of the T-loop (as above, 157 to 172) were within 1.02 Å (RMSD) of the corresponding atoms in ERK2.

The residues used to generate a predicted α_c helix differed slightly for the two templates. CDK2 has a helix-breaking leading proline in PSTAIRE and a shorter 11-residue α_c helix. However, ICK does not have this proline. ICK residues 45 to 55 in this model were used to form an 11-residue α_c helix on the CDK2 template. ERK2 has a longer α_c helix of 15 residues. Residues 46 to 56 were superimposed on a portion of the 15-residue α_c helix in ERK2.

Phosphorylation within the TDY motif is required for activity. ICK has autokinase and MBP phosphotransferase activities (40). We expressed GST-ICK and mutant proteins in HEK293T cells for activity assay (Fig. 2A). Incorporation of ^{32}P into ICK is catalyzed by ICK, because no incorporation was detectable within a kinase-dead K33R mutant (Fig. 2A). ICK ADY, TDF, and ADF mutants of the TDY motif were inactive in both autophosphorylation and MBP phosphorylation, suggesting that both T and Y in the TDY motif are required for autokinase activity and MBP phosphotransferase activity.

To implicate the TDY motif as the site of regulatory phosphorylation, we used an anti-phosphoERK antibody. Anti-phosphoERK detected ICK (Fig. 2B), strongly implying that ICK is phosphorylated within its TDY motif. This antibody reacted very weakly with the ADY mutant and had no detectable cross-reactivity with the TDF mutant, suggesting that it reacts much more strongly with the dually phosphorylated TDY motif. Significantly, a K33R mutant lost the Western blot signal, implying that TDY phosphorylation requires autokinase activity. Treatment with PP2A, which is Ser/Thr specific, significantly reduced the anti-phosphoERK signal and MBP phosphotransferase activity of ICK (Fig. 2C). Therefore, ICK activity is regulated by threonine phosphorylation within the TDY motif. In Fig. 2C, it is worth of pointing out that a 60-kDa band was enriched after PP2A treatment in parallel with a decrease in the protein level of full-length GST-ICK. This band was recognized by both anti-phosphoERK and anti-ICK(N), as well as anti-ICK(C) (data not shown). We suspect the proteolysis probably occurs in the GST tag or very near the N terminus of ICK, as the anti-ICK(N) is to ICK residues 46 to 56. Inhibition of PP2A clearly prevented dephosphorylation of the TDY motif in both the full-length GST-ICK and the 60-kDa cleavage product.

Dual phosphorylation of ICK on the TDY motif in cells. We used targeted-mode mass spectrometry to determine if TDY phosphorylation of ICK occurs in cells. Of the three potential forms, the nonphosphorylated peptide ($[M + 2H]^{2+} = m/z$ 721.7) was the most abundant based on peak area (data not shown). The $[M + 2H]^{2+}$ ions of the doubly phosphorylated (m/z 801.8) and singly phosphorylated (m/z 761.7) peptides were also readily detected but at an order of magnitude lower than the nonphosphorylated form. Interpretation of the MS/MS spectrum for m/z 801.8 revealed conclusive b/y-type fragment ions that defined its phosphorylation on both threonine and tyrosine (T*DY*) (Fig. 2D), whereas the fragmentation pattern of the singly phosphorylated form (m/z 761.7) indicated phosphorylation on the tyrosine (TDY*) (Fig. 2E). The latter spectrum had an identical fragmentation pattern as synthesized SRPPYTDY*VSTR peptide, suggesting that there was no significant contribution from other potentially coeluting isoforms (data not shown). In addition, mass spectrometry showed that PP2A treatment completely abolished the dually phosphorylated form, leaving only the singly phosphorylated form (data not shown). We conclude that a portion of ICK in unstimulated and asynchronized HEK293T cells is dually phosphorylated on the TDY motif.

GFP-ICK but not GFP-ICKb is nuclear. The human ICKb variant (accession number AAH35807) is identical to human ICK in amino acids 1 to 277 and may use an alternative 5′ noncoding exon and an alternative splice site in the 3′ coding region to introduce alternative codons for 15 unique amino acids and then a stop codon. Thus, the encoded isoform b has 292 amino acids and a shorter, distinct C terminus (see Fig. 4E). To assess cellular localization, we expressed mouse ICK or human ICKb with a green fluorescence protein (GFP) tag fused to the N terminus (Fig. 3A). GFP-ICK expressed in COS-7 cells localized predominantly to the nucleus (44) (Fig. 3B). In contrast, GFP-ICKb was predominantly in the cytoplasm (Fig. 3B). Predominant steady-state nuclear localization of ICK does not exclude the possibility that ICK shuttles between these two compartments.

Nuclear localization of ICK does not require kinase activity or TDY phosphorylation. Both the K33R and the ADF mutant localized to the nucleus (Fig. 3C). Thus, kinase activity and TDY phosphorylation of ICK are not required for nuclear targeting. The noncatalytic domains of some of the large ERKs (ERK7 [3] and ERK5 [43]) are required for nuclear localization. Given that amino acids 1 to 277 of ICK and ICKb are identical, the cytoplasmic localization of ICKb suggests that residues 278 to 629 of ICK are important for nuclear localization.

Subdomain XI is required for nuclear localization and kinase activity. To survey the C-terminal domain of ICK, we constructed a series of truncation mutants as GFP fusions (Fig. 4A). Progressive truncations of the C terminus of GFP-ICK did not alter nuclear localization until there was a dramatic contrast between constructs GFP-ICK(1–277) and GFP-ICK(1–300) (Fig. 4A). GFP-ICK(1–300) is predominantly nuclear, whereas GFP-ICK(1–277) is predominantly cytoplasmic. The same mutants were generated as GST fusions to assay activity. Truncation mutants in the first series were kinase active until residues 278 to 300 were deleted, as assayed by either autokinase activity (Fig. 4B, top) or reactivity with anti-phosphoERK antibody (Fig. 4B, middle). Loss of kinase activity for ICK(1–277) was not due to loss of expression, as demonstrated by Western blotting with anti-GST antibody (Fig. 4B, bottom).

Figure 4E shows a schematic of subdomain XI in ICK. Residues 278 to 300 overlap the end of subdomain XI (13). Subdomain XI contains a predicted α_h helix and a shorter α_i helix. The cytoplasmic localization of variant ICKb is not due to the residue substitutions in the C-terminal end of ICKb. Rather, ICKb and ICK(1–277) are both disrupted within the predicted α_i helix ASQAL in subdomain XI after Q. Thus, an intact α_i helix is required for both nuclear localization and kinase ac-

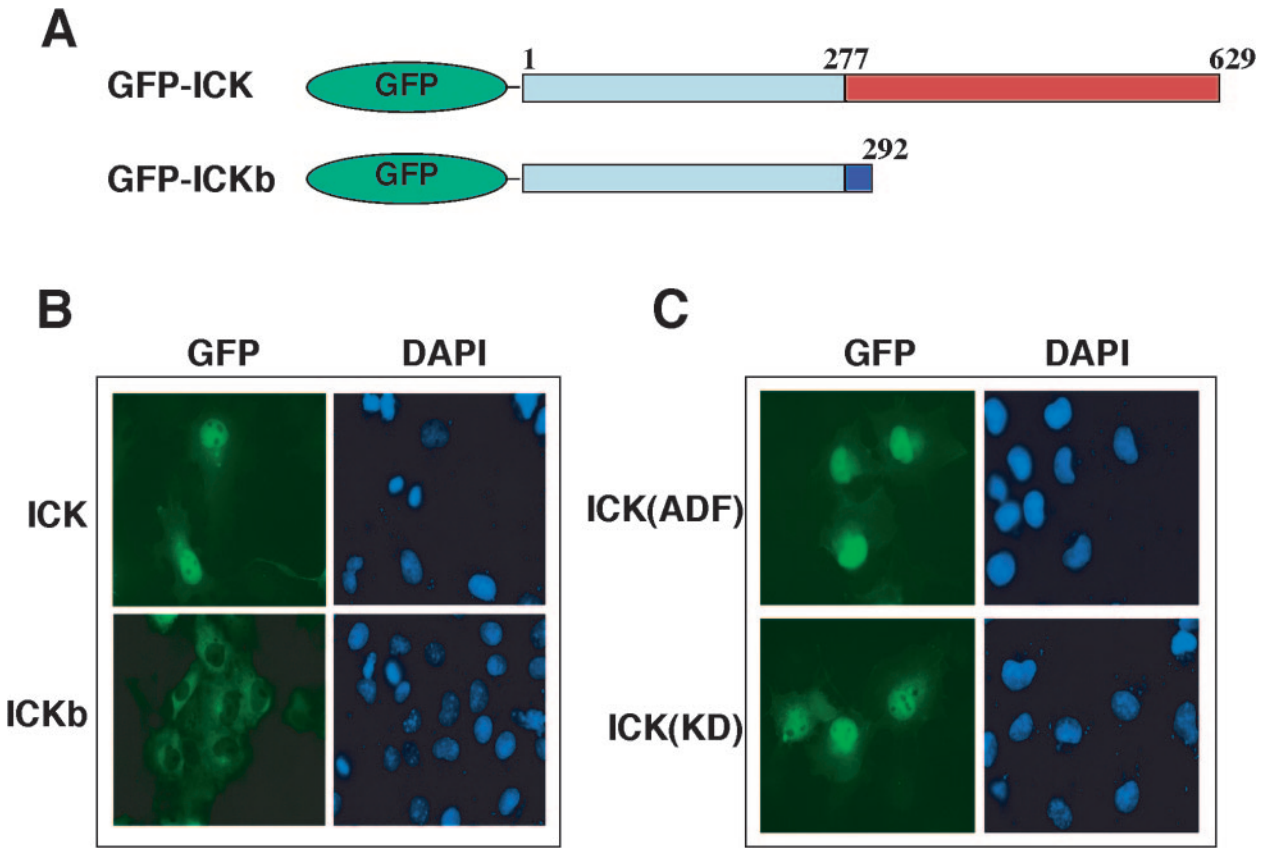

FIG. 3. ICK is nuclear, and neither the kinase activity nor the TDY motif phosphorylation is required for its nuclear localization. (A) Schematic diagram of GFP-ICK and GFP-ICKb constructs. Note that ICK and ICKb are identical at amino acids 1 to 277 in the catalytic domain but differ in the length and composition of the C-terminal domain. (B) Immunofluorescence of GFP-ICK and GFP-ICKb in COS-7 cells. Shown are GFP staining for ICK (left panel) and DAPI staining for the nucleus (right panel). (C) Immunofluorescence of GFP-ICK(KD) and GFP-ICK(ADF) mutants in COS-7 cells, shown as in panel B.

tivity. Prp4p, a regulator of splicesomes, is more distantly related to MAPKs and CDKs. Mutations demonstrated that the α_i helix in subdomain XI is required for Prp4p function (28).

To refine the requirements, we made truncations within residues 278 to 300 (Fig. 4E). Truncation after residue 291 removes the entire noncatalytic domain, and the GFP-fusion, surprisingly, remains nuclear (Fig. 4D). GFP-ICK(1–284), which is truncated to the boundary of subdomain XI (YPYF in ICK), is also nuclear. ICK(1–277) and ICKb are completely inactive and do not detectably immunoblot with anti-phosphoERK antibody (Fig. 4B) whereas ICK(1–284) and the longer mutant ICK(1–291) retain reactivity (Fig. 4C).

Nuclear localization and kinase activity require R272. No putative nuclear localization sequence is present in the α_i sequence. In modeled ICK as well as CDK2 and ERK2 structures, α_i interacts with α_h. Conceivably, truncation of α_i [mutant ICK(1–277)] disrupts the interaction between α_i and α_h, thus destabilizing the structure of L15. The conserved arginine, R272, is in a PKKRP motif in L15 (Fig. 4E). Therefore, we hypothesized that R272 plays a key role in nuclear localization, and we tested this by mutating the PKKRP motif.

Full-length GFP-ICK mutants singly (K270A, K271A) or doubly (K270A/K271A) mutated in the lysines in the motif were nuclear (Fig. 5B). However, the triple mutant K270A/K271A/R272A caused localization outside the nucleus (Fig. 5B). Indeed, a single R272A point mutation was sufficient to cause loss of nuclear localization (Fig. 5B). The mutants K270A, K271A, and K270A/K271A each had reduced but readily detectable autokinase activity and reactivity to anti-phosphoERK in comparison to the wild type (Fig. 5A). In contrast, the triple mutant of K270/K271/K272 and the single R272A mutant were as kinase inactive as the K33R kinase-dead mutant (Fig. 5A, top panel). Neither had reactivity to anti-phosphoERK antibody (Fig. 5A, bottom panel).

Thus, subdomain XI is required for both kinase activity and nuclear localization of ICK. It should be emphasized that mutants K33R and ADF, both of which cause kinase inactivation, retain nuclear localization (Fig. 3C). These residues are distant from subdomain XI and serve to dissociate kinase activity and nuclear localization.

Modeling of subdomain XI. One function of the conserved arginine is the stabilization of the large lobe by formation of an ion pair with the conserved glutamate residue in the APE motif at the end of the T loop (13). In ICK modeled to ERK2 (Fig. 1C, right), R272 was positioned to form the expected ion pair to E169 (Fig. 5E). In ICK modeled to CDK2 templates (Fig. 1C, left), this was not the case, suggesting that ERK2 may well be the better structural template in this region. The side chains

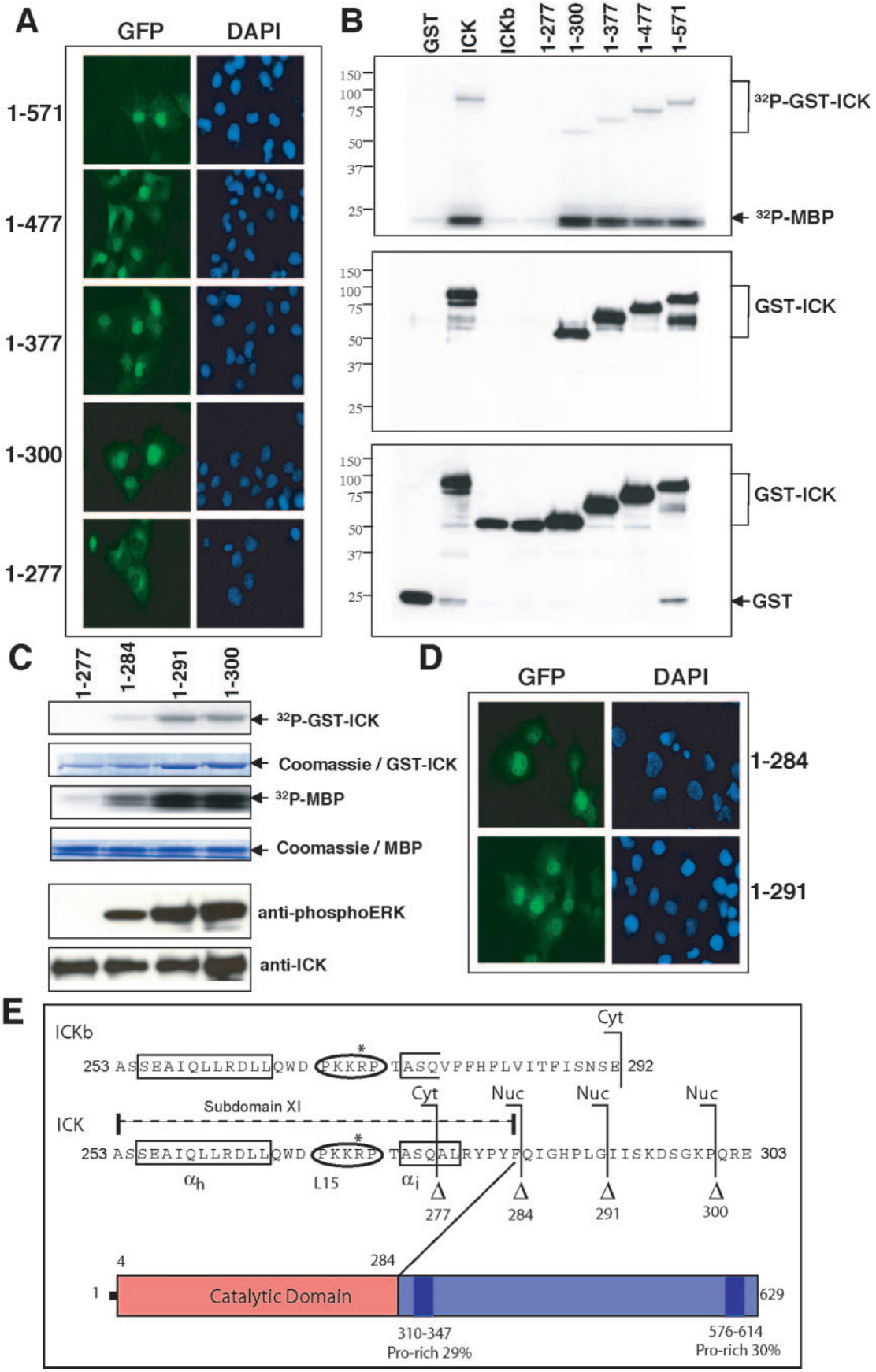
A
GFP
DAPI
1-571
1-477
1-377
1-300
1-277
B
GST
ICK
ICKb
1-277
1-300
1-377
1-477
1-571
150
100
75
50
37
25
32P-GST-ICK
32P-MBP
GST-ICK
GST-ICK
GST
C
1-277
1-284
1-291
1-300
32P-GST-ICK
Coomassie / GST-ICK
32P-MBP
Coomassie / MBP
anti-phosphoERK
anti-ICK
D
GFP
DAPI
1-284
1-291
E
ICKb
253 ASSEAIQLLRDLLQWD PKKRP TASQVFFHFLVITFISNSE 292
Cyt
ICK
Subdomain XI
253 ASSEAIQLLRDLLQWD PKKRP TASQALRYPYFQIGHPLGIISKDSGKPQRE 303
αh
L15
αi
Cyt
Nuc
Nuc
Nuc
Δ 277
Δ 284
Δ 291
Δ 300
4
284
1
Catalytic Domain
629
310-347
Pro-rich 29%
576-614
Pro-rich 30%

of K270 and K271 are exposed in this ICK model. Although the guanidinium side chain of R272 in the model is not exposed, the R272 backbone is partially exposed on the surface. Similarly, the backbones of the subdomain XI arginine in human CDK2 (R274) and in rat ERK2 (R299) are partially exposed in a pocket with an oxygen atom exposed (data not shown). R272 may be required to create a conformation or binding surface that is essential for nuclear localization.

Network of interactions of R272 is required. To confirm the critical role for R272, we generated mutations at E169 and W184 predicted to interact with R272. Residue E169 should make an ion pair with R272. Residue W184 should be positioned to stabilize the ion pair formed between E169 and R272. W184 occurs in a highly conserved DIW motif in the predicted F helix. In the structure of the C subunit of cyclic AMP-dependent protein kinase, this tryptophan is positioned to stabilize the ion pair between residues equivalent to R272 and E169 (13). The E169A mutant was cytoplasmic (Fig. 5D), establishing the same functional effect as for R272A by the reciprocal disruption of the ion pair. W184A, predicted to alter contacts with R272, was also cytoplasmic (Fig. 5D). Similar to the R272A mutant, both the E169A and W184A mutants are kinase inactive (Fig. 5C, top) and did not react with anti-phosphoERK antibody (Fig. 5C, bottom).

ICK expressed in *E. coli* is reactive with anti-phosphoERK antibody. In prokaryotic cells, reconstitution of protein kinase activation can be a test for sufficiency of introduced components. ERK7 autokinase activity was reported to be sufficient for dual TEY phosphorylation in *E. coli* (2). Additions of growth factors did not detectably augment ICK autokinase activity (40), another parallel to ERK7. With these motivations, we next compared phosphorylation and activity of HEK- and *E. coli*-expressed ICK.

Full-length ICK could not be expressed in *E. coli* (data not shown). This may be due to the presence of several segments of low compositional complexity in the C-terminal domain of ICK predicted by SMART analysis (34). However, several constructs of ICK that we tested expressed well in both cellular systems, permitting comparison. ICK(1–284), ICK(1–291), and ICK(1–300) were reactive with anti-phosphoERK antibody whether expressed in eukaryotic or prokaryotic cells (Fig. 6A, top panel). ICK(1–277) is kinase dead and served as an internal control for phosphospecificity. Lack of reactivity was not due to absence of protein, as protein amounts were similar by anti-GST Western blotting (Fig. 6A, bottom panel). Since *E. coli* does not express endogenous protein serine/threonine or tyrosine kinases, ICK kinase activity is sufficient for phosphorylation to occur within the TDY motif.

ICK expressed in *E. coli* has much lower specific activity. ICK(1–284), ICK(1–291), and ICK(1–300) expressed in mammalian cells were strikingly more active when assayed by autokinase activity or MBP phosphorylation (Fig. 6B). Activities were normalized for protein to compare specific activities for ICK autokinase activity (Fig. 6C) or MBP phosphotransferase activity (Fig. 6D). ICK obtained from HEK293T cells is 5 to 10-fold more active. Both *E. coli*- and HEK293T-expressed ICK proteins were soluble. Nevertheless, an unknown difference in protein folding might be a caveat for this difference. Our prior work on p42 MAPK/ERK2 suggested another possibility for the marked difference in specific activity: ICK from *E. coli* might lack threonine phosphorylation within the TDY motif (27).

Dual phosphorylation of ICK on TDY occurs in HEK293T cells but not in *E. coli*. We analyzed site phosphorylation of ICK(1–300) by mass spectrometry. The ion abundances from a targeted analysis of the TDY tryptic peptides are shown in Fig. 6E. Only the nonphosphorylated peptide, SRPPYTDYVSTR (*m*/*z* 721.7), and the tyrosine-phosphorylated peptide, SRPPY TDY*VSTR (*m*/*z* 761.7), were detected in the digest from ICK(1–300) from *E. coli* (left panel). In contrast, these two forms and the doubly phosphorylated peptide, SRPPYT*DY *VSTR (*m*/*z* 801.7), as well as an unanticipated serine-phosphorylated peptide, SRPPYTDYVS*TR, were detected in digests from HEK293T cells (right panel). Only the nonphosphorylated tryptic TDY peptide was present in kinase-dead ICK(1–277) expressed in either *E. coli* or HEK293T cells (data not shown). Reactivity of ICK(1–300) from *E. coli* with anti-phosphoERK is abolished by *Yersinia* protein tyrosine phosphatase as well as λ protein phosphatase (Fig. 6F). This result establishes that the tyrosine phosphorylation in the TDY motif of ICK(1–300) from *E. coli* is reversible and sufficient for recognition by anti-phosphoERK. However, the predominant reactivity to TDY over the ADY mutant (Fig. 2B) and the near-complete loss of immunostaining after PP2A treatment (Fig. 2C) establish that anti-phosphoERK reacts much more strongly with dually phosphorylated ICK.

Thus, ICK(1–300) autophosphorylates on the tyrosine residue of the TDY motif in *E. coli* but not detectably on the threonine residue. The latter is similar to $p42^{MAPK}$/ERK2, which autophosphorylates on tyrosine but not threonine at TEY (41). Our mass spectrometry data strongly suggest that the cross-reactivity of *E. coli*-obtained ICK(1–300) in Fig. 6A is due to retained cross-reactivity of the antibody to tyrosine-phosphorylated TDY motifs. The absence of doubly phosphorylated TDY peptide in ICK(1–300) from *E. coli* is sufficient to explain its lower specific activity, although we cannot exclude

FIG. 4. Subdomain XI is required for nuclear targeting and kinase activity. (A) Immunofluorescence of the serial C-terminal truncations of ICK in COS-7 cells, with GFP staining for ICK and DAPI staining for the nucleus. (B) In vitro kinase assay using full-length ICK and ICKb as well as the serial C-terminal truncations of ICK. The assay was done as described for Fig. 2A. Shown are the autoradiograph (top panel) and Western blots of an equal portion of the bead sample against anti-phosphoERK antibody (middle panel) and anti-GST antibody (bottom panel). (C) In vitro kinase assay using two additional ICK C-terminal truncation mutants, ICK(1–284) and ICK(1–291). The assay was done as for panel B. Shown are the autoradiograph (top panel) and Western blots of an equal portion of the bead sample against anti-phosphoERK antibody and anti-GST antibody (bottom panel). (D) Immunofluorescence of GFP-ICK(1–284) and GFP-ICK(1–291) in COS-7 cells, with GFP staining for ICK and DAPI staining for the nucleus. (E) Schematic diagram of ICK subdomain XI aligned with the C-terminal sequence of ICKb, highlighting residue 284, after which the C-terminal truncation of ICK maintains a basic level of kinase activity and is still nuclear. Note the presence of a basic PKKRP motif in the L15 sequence that contains the conserved Arg-272.

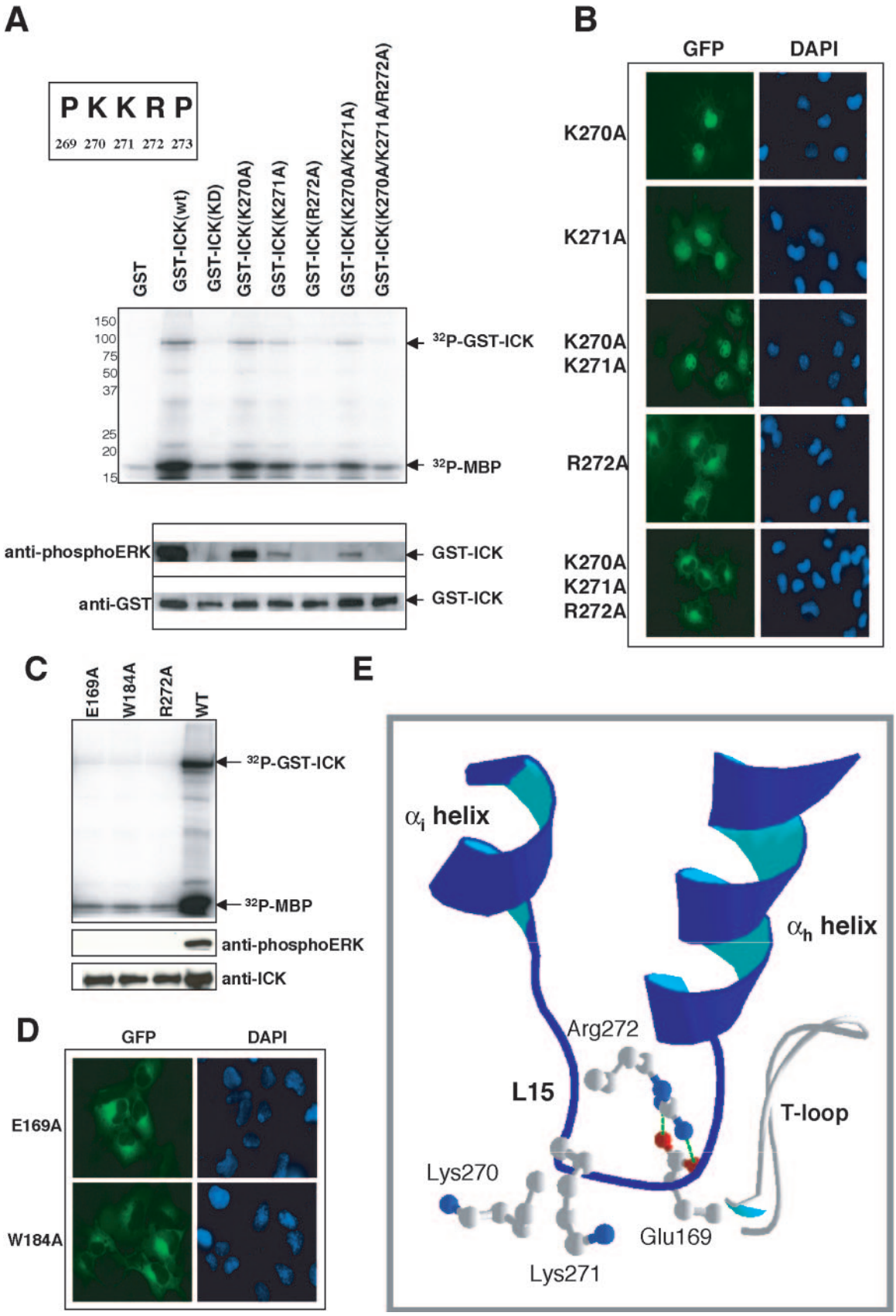
A
P K K R P
269 270 271 272 273
GST
GST-ICK(wt)
GST-ICK(KD)
GST-ICK(K270A)
GST-ICK(K271A)
GST-ICK(R272A)
GST-ICK(K270A/K271A)
GST-ICK(K270A/K271A/R272A)
150
100
75
50
37
25
20
15
32P-GST-ICK
32P-MBP
anti-phosphoERK
GST-ICK
anti-GST
GST-ICK
B
GFP
DAPI
K270A
K271A
K270A K271A
R272A
K270A K271A R272A
C
E169A
W184A
R272A
WT
32P-GST-ICK
32P-MBP
anti-phosphoERK
anti-ICK
D
GFP
DAPI
E169A
W184A
E
αi helix
αh helix
Arg272
L15
T-loop
Lys270
Glu169
Lys271

the possibility that other phosphorylation sites (such as pS161 [Fig. 6E, right panel]) present in ICK(1–300) from HEK293T cells may also be important. Our data are consistent with a model in which dual phosphorylation of ICK on threonine and tyrosine requires a cellular activator(s).

Activation of ICK requires nuclear targeting. To determine if the cellular activator(s) may be nuclear, we generated constructs to express ICK proteins having an added nuclear export sequence (NES-ICK) (Fig. 7A). GFP-NES-ICK was excluded from the nucleus (Fig. 7B). We assayed relocated proteins for activity (Fig. 7C). ICK was inactivated by nuclear exclusion. The ICK wild-type control had autokinase activity above background, whereas NES-ICK did not. It should be noted that a ^{32}P band running well above the position of wild-type ICK is not NES-ICK, as proven by overlay with the Coomassie blue-stained gel. This background band was observed in all lanes. K33R and R272A mutants were kinase dead and served as controls for autokinase activity. Thus, nuclear localization appears to be required for full activation of ICK.

CAK, but not MEK, phosphorylates and activates ICK. Since the catalytic domain of ICK is similar to those of both ERK2 and CDK2, we tested whether the ERK2 activator MEK or the CDK2 activator CAK activates ICK. In Fig. 8, either constitutively active MEK1 [MEK1(DD)] or constitutively active MEK5 [MEK5(DD)] was coexpressed with ICK in HEK293T cells. As controls, MEK1(DD) was separately coexpressed with ERK2 and MEK5(DD) was separately coexpressed with ERK5. Both controls worked well, as the MBP phosphotransferase activity and the anti-phosphoERK reactivity of ERK2 and ERK5 were increased significantly in the presence of MEK1(DD) or MEK5(DD), respectively. However, neither MEK1(DD) nor MEK5(DD) triggered any detectable increase of either MBP phosphotransferase activity or anti-phosphoERK reactivity of ICK. This result indicates that MEK does not phosphorylate ICK in the T loop and thus is not the upstream activator of ICK.

We then tested CAK, an activator that is required for T-loop phosphorylation in many CDKs. Two classes of CAKs have been well characterized so far: monomeric Cak1p from budding yeast and $p40^{MO15}$(CDK7)/cyclin H/MAT1 complex from human (14). Monomeric Cak1p is active in the absence of a cyclin and can be produced as a potent homogeneous, recombinant CAK. Both Cak1p and $p40^{MO15}$ complex activate CDKs by phosphorylating the same residue (equivalent to Thr-160 in human CDK2), although via different enzyme-substrate recognition mechanisms (16). We asked whether CAK phosphorylates ICK at Thr-157 in the T loop, equivalent to Thr-160 in human CDK2. Since *E. coli*-expressed ICK(1–300) but not HEK293T-expressed ICK lacks phosphate on Thr-160 in the T loop, we chose to test *E. coli*-expressed ICK(1–300) as a substrate for phosphorylation by CAK. To enable site identification and comparisons, the TDY motif in the T loop of ICK(1–300) was mutated to generate the ADF, ADY, and TDF mutants. As shown in Fig. 9A, the wild-type TDY and the mutant ADY, but not the ADF and TDF mutants, can autophosphorylate in the absence of CAK and react to anti-phosphoERK antibody, suggesting that Tyr-159 is required for autophosphorylation. However, unlike the wild-type TDY, the mutant ADY cannot phosphorylate MBP, indicating that both Thr-157 and Tyr-159 are required for full kinase activity. The wild-type TDY and its mutants then were individually incubated with purified recombinant Cak1p for in vitro phosphorylation (Fig. 9B). There was a significant increase in the phosphorylation levels of both the wild-type TDY and the TDF mutant after Cak1p and ATP/Mg treatment. This increase was totally abolished in the ADY and ADF mutants due to the Thr-Ala mutation, proving that the major site of phosphorylation by Cak1p in the wild-type TDY and the TDF mutant is Thr-157.

A time course for phosphorylation by Cak1p was determined for both *E. coli*-expressed ICK(1–300) and HEK293T-expressed ICK(1–300) substrates (Fig. 9C). The ^{32}P incorporation into *E. coli*-expressed ICK(1–300) was dramatically increased by Cak1p even at earlier time points (15 and 30 min) (Fig. 9C, top panel). In contrast, ^{32}P incorporation into HEK293T-expressed ICK(1–300) by Cak1p was very slow, and an increase of about twofold was achieved only at a later time point (60 min) (Fig. 9C, bottom panel). By mass spectrometry (Fig. 6E), about 40% of the TDY peptide in *E. coli*-expressed ICK(1–300) is singly tyrosine phosphorylated and the rest (60%) is unphosphorylated, whereas only about 10% of the TDY peptide in HEK293T-expressed ICK(1–300) is singly tyrosine phosphorylated and about 80% is unphosphorylated. Therefore, the difference in stoichiometry of Cak1p phosphorylation between *E. coli*-expressed and HEK293T-expressed ICK(1–300) can be rationalized if the singly tyrosine-phosphorylated ICK is the preferred substrate. The *E. coli*-expressed ICK(1–300) was then used for assessing the effect of Cak1p phosphorylation on ICK activity.

We asked whether the Thr-157 phosphorylation by CAK would increase the kinase activity of ICK. Beads with *E. coli*-expressed ICK(1–300) samples were treated with Cak1p as described for Fig. 9B except with only nonradioactive ATP. After reaction, bead samples were extensively washed in kinase buffer to remove Cak1p and assayed for in vitro phosphorylation of MBP (Fig. 9C). Significantly, Thr-157 phosphorylation

FIG. 5. The conserved R272 in the PKKRP motif and its interactions with both E169 and W184 are crucial for both nuclear localization and kinase activity. (A) In vitro kinase assay using the PKKRP motif mutants. Basic residues were mutated to alanine. The mutants were expressed in HEK293T cells and assayed for kinase activity (top panel) and for reactivity to anti-phosphoERK and anti-GST antibodies (bottom panel). (B) Immunofluorescence of the PKKRP motif mutants. The set of ICK mutants used for panel A were subcloned into pEGFP-C3 vector and transfected into COS-7 cells. Shown are GFP staining for ICK and DAPI staining for the nucleus. (C) In vitro kinase assay using E169A and W184A mutants. Shown are the autoradiograph (top panel) and the Western blots against anti-phosphoERK and anti-ICK(C) antibodies (bottom panel). (D) Immunofluorescence of GFP-ICK(E169A) and GFP-ICK(W184A) mutants. Shown are GFP staining for ICK and DAPI staining for the nucleus. (E) Structure of subdomain XI of ICK from a SwissModel model to ERK2. The PKKRP motif is located in L15. The interface of α_h-L15-α_i may help to create an active conformation that is required for both nuclear targeting and kinase activity. In ICK modeled to ERK2, R272 makes an ion pair with E169 in the T loop and interacts with W184 (not shown).

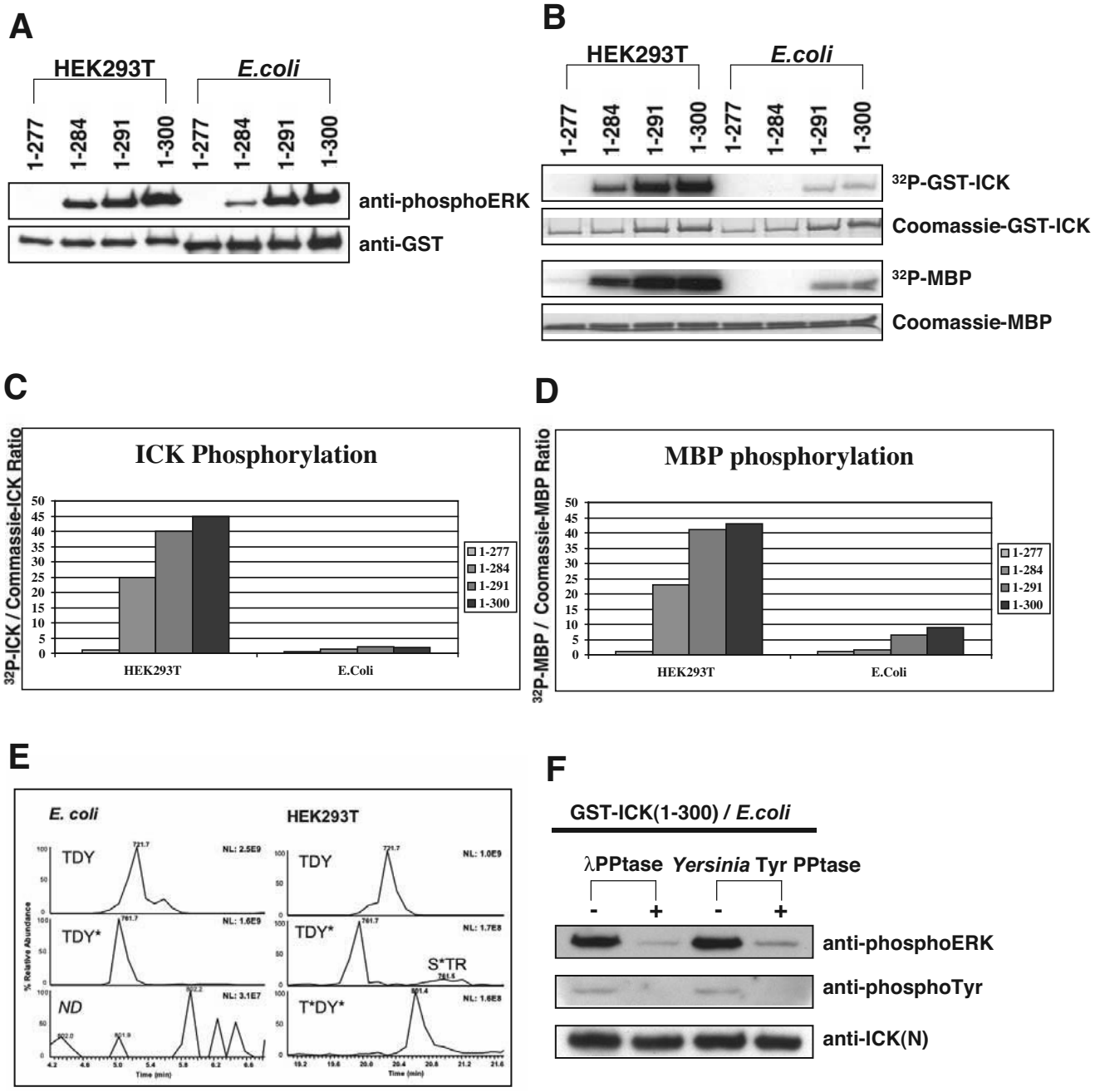

FIG. 6. *E. coli*-expressed ICK has much lower specific activity than HEK293T-expressed ICK and is not doubly phosphorylated within the TDY motif. (A) Western blot of GST-ICK truncation mutants expressed in either HEK293T cells or *E. coli* against anti-phosphoERK and anti-GST antibodies. (B) Autoradiograph of in vitro kinase assay using GST-ICK truncation constructs expressed in either HEK293T cells or *E. coli*. Also shown are Coomassie blue-stained GST-ICK and MBP bands in SDS gel. (C) Quantitation of ICK autophosphorylation shown in panel B. (D) Quantitation of MBP phosphorylation shown in panel B. (E) Comparison of selected ion chromatograms from MS targeted analysis of tryptic peptides containing the TDY motif from GST-ICK(1–300) expressed in *E. coli* or HEK293T cells. Note that no MS/MS spectra were recorded for the T*DY* peptide from *E. coli*, and the most abundant signal in this chromatographic window (3.1E7) is approximately an order of magnitude lower than that of the T*DY* peptide from HEK293T cells (1.6E8). (F) *E. coli*-expressed GST-ICK(1–300) was treated with either λ protein phosphatase (PPtase) or *Yersinia* protein tyrosine phosphatase and analyzed by immunoblotting with anti-phosphoERK (top panel) and antiphosphotyrosine (4G10) (middle panel). Anti-ICK(N) (bottom panel) indicates the overall expression level of ICK.

by Cak1p increased the autokinase activity and MBP phosphotransferase activity of *E. coli*-expressed ICK(1–300). As a control, the residual amount of Cak1p left on the beads after washing did not phosphorylate MBP (data not shown).

To test whether ICK could be phosphorylated and activated by CAK1 in vivo, full-length GST-ICK or GST-ICK(1–300) was coexpressed with wild-type CAK1 or inactive mutant CAK1(N161A) in HEK293T cells (Fig. 10). Coexpression of

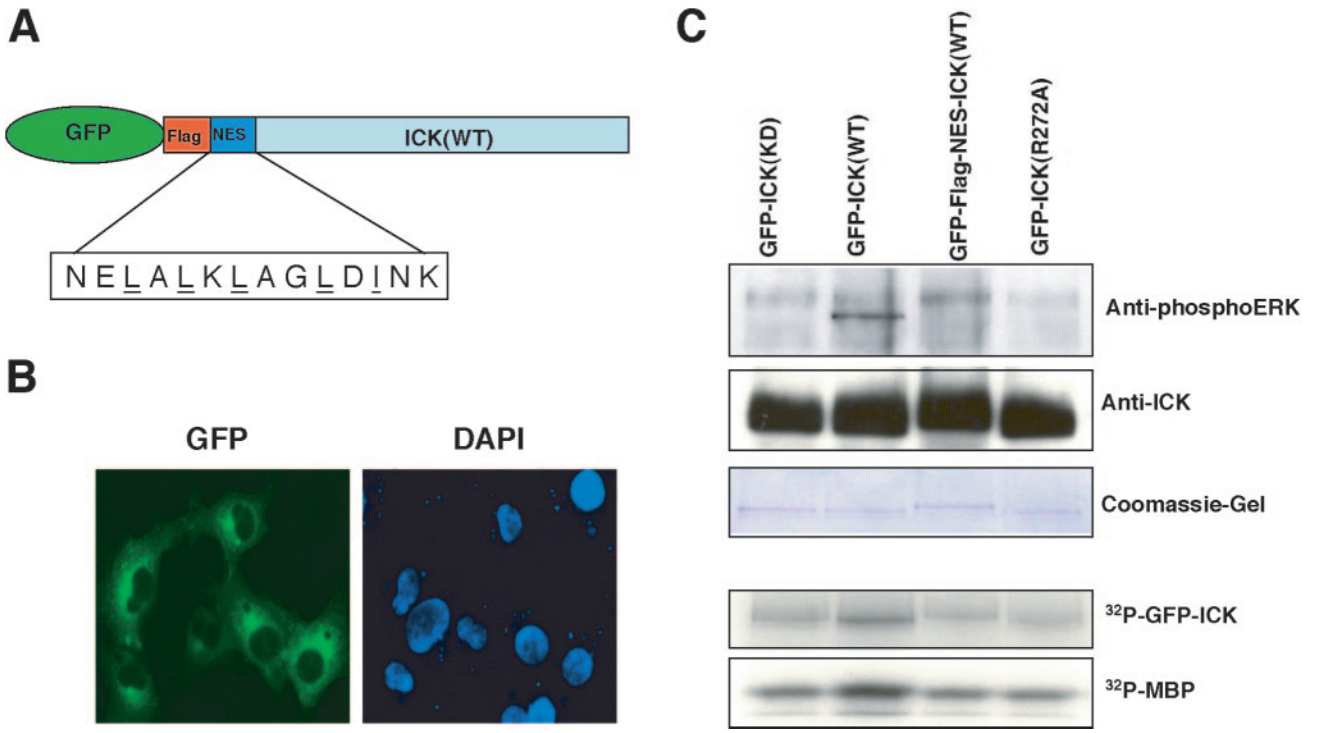

FIG. 7. Activation of ICK requires nuclear targeting. (A) Schematic of the GFP-Flag-NES-ICK. (B) Immunofluorescence of GFP-Flag-NES-ICK in COS-7 cells. Shown are GFP staining for NES-ICK (left panel) and DAPI staining for the nucleus (right panel). (C) Kinase assay of GFP-Flag-NES-ICK. The GFP fusion proteins were expressed in HEK293T cells and immunoprecipitated with anti-GFP. The immune complex was pulled down with protein A-agarose beads. Equal portions of the beads were assayed for either reactivity to anti-phosphoERK and anti-ICK(C) antibodies (Western blot, top panel) or kinase activity (autoradiograph, bottom panel). Also shown in the top panel is the Coomassie blue-stained SDS gel containing equal portions of the beads used for the Western blot.

CAK1(WT), but not the CAK1(N161A) mutant, triggered a significant increase in the anti-phosphoERK reactivity signal for both full-length ICK and ICK(1–300), suggesting that CAK1(WT) phosphorylates ICK in the TDY motif in vivo (Fig. 10A). As a control, the anti-phosphoERK signal against ERK2 containing the TEY motif was not affected by CAK1(WT) (Fig. 10A), implying that CAK1(WT) phosphorylation of ICK in the TDY motif does not apply to all TXY motif kinases but is in some measure specific to ICK. Coexpression of CAK1(WT), but not CAK1(N161A), also caused about a twofold increase in autophosphorylation and MBP phosphorylation of full-length ICK (Fig. 10B and C), indicating that CAK1(WT) phosphorylation of ICK in the TDY motif activates its autokinase and MBP phosphotransferase activities. In contrast, the autokinase and MBP phosphotransferase activities of ERK2 were not significantly altered by CAK1(WT) (Fig. 10B and C). This result is consistent with our in vitro observation that Cak1p did not phosphorylate *E. coli*-expressed recombinant ERK2 (data not shown). The twofold increase of ICK kinase activity by CAK1 phosphorylation in HEK293T cells is consistent with the stoichiometry of the phosphorylated TDY peptide predicted from mass spectrometry of the HEK293T-expressed ICK(1–300) sample, in that about 10% of the TDY peptide is singly tyrosine phosphorylated and another 10% is dually phosphorylated (Fig. 6E, right panel).

Thus, we conclude that CAK, but not MEK, activates ICK by phosphorylating Thr-157 in the T loop.

DISCUSSION

In summary, ICK is the prototype for a novel group of mammalian kinases regulated by dual phosphorylation of TDY motifs. We show unequivocally that ICK is phosphorylated at TDY and that dual phosphorylation correlates with full kinase activity. Autokinase activity may account for the tyrosine phosphorylation in the TDY motif. Tyrosine phosphorylation is required for the basal kinase activity of ICK. However, additional phosphorylation of the threonine residue in the T loop by CAK is required for full kinase activity.

Yeast CAK can serve as a T157 kinase, suggesting a mammalian CAK may emerge as a physiologic ICK activator. The presence of two different kinds of CAK activities from human cells has been suggested (17). In addition to the CDK7/cyclin H/MAT1 complex, a peak of CAK activity at 30 to 40 kDa also exists, and its activity resembles that of yeast Cak1p rather than CDK7 complex in terms of substrate specificity and antibody reactivity. Furthermore, a novel CAK p42 was identified in mammalian cells, which shares sequence homology to both Cak1p and CDK7 (22). Whether either of these CAKs is a physiologic T157 kinase for ICK remains to be determined. In yeast, Cak1p is dispersed throughout the cells (15). In mammalian cells, both CDK7 and p42 are nuclear proteins (14), which is consistent with the observation that nuclear localization is required for ICK kinase activity.

PP2A inactivates ICK by dephosphorylation of threonine in

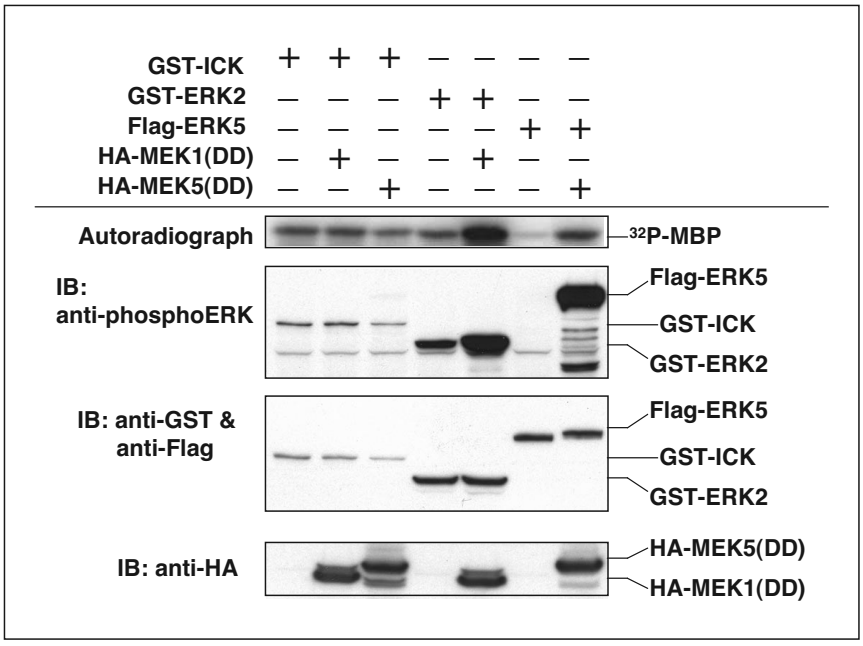

FIG. 8. Unlike ERKs, constitutively active MEKs cannot further activate ICK. GST-ICK, GST-ERK2, or Flag-ERK5 was cotransfected with either constitutively active HA-MEK1(DD) or constitutively active HA-MEK5(DD) in HEK293T cells. From cell lysate, GST-ICK and GST-ERK2 were pulled down with glutathione-Sepharose beads, whereas Flag-ERK5 was pulled down with anti-Flag M2 monoclonal antibody followed by protein A-agarose beads. After extensive washing, equal amounts of beads were subjected to either in vitro kinase assay (autoradiograph shown in the upper panel) or immunoblot (IB) analysis (Western blots shown in the middle panels). Total cell lysate was blotted with anti-HA (bottom panel) to show the expression of HA-tagged MEK1(DD) and MEK5(DD).

the TDY motif. ICK(1–300) expressed in *E. coli* is only significantly phosphorylated in the TDY motif on the tyrosine, and treatment of *E. coli* ICK(1–300) with either λ phosphatase or *Yersinia* protein tyrosine phosphatase eliminates anti-phosphoERK2 reactivity (Fig. 6F). This suggests that tyrosine phosphorylation is regulatory in this lower-specific-activity form. In addition, ICK(1–300) from *E. coli* is about fivefold less active than ICK(1–300) from HEK293T cells, which is dually phosphorylated on the TDY motif. Further, a TDF mutant of ICK is as kinase dead as K33R or ADF. Thus, these data support our conclusion that tyrosine as well as threonine phosphorylation of ICK is regulatory. MAK is predicted to have similar regulation.

Some observations we made are helpful for defining a mechanism of ICK activation. First, K33R ICK expressed in HEK293T cells is not only kinase defective but also not detectably phosphorylated on the TDY motif. This establishes that autokinase activity is required for ICK activation. ICK(1–300) expressed in *E. coli* is tyrosine phosphorylated but not threonine phosphorylated in the TDY motif. The latter is reminiscent of an ability of ERK2 to autophosphorylate on tyrosine. Autophosphorylation of ERK2 on tyrosine is a slow reaction, and our assays suggest that ICK tyrosine autophosphorylation is similarly slow (data not shown). Thus, there may exist a specific complex or context in cells that enhances autokinase activity at Y159 or even broadens autokinase activity to include T157. A precedent for the latter is Tab1-stimulated autophosphorylation of p38α MAPK on both threonine and tyrosine sites in the TGY motif (11). The absence of T157 phosphorylation in *E. coli* indicates a requirement for an upstream kinase and/or allosteric factors. It is possible that there is a nuclear T157 kinase for ICK. Our data suggest a nuclear CAK as the leading candidate. Alternatively, a nuclear MEK-like activity other than MEK1 or MEK5 with dual specificity for TDY could be involved. For example, Crk1 is a TEY motif kinase in the plant pathogen *Ustilago maydis* that is closely

FIG. 9. CAK phosphorylates ICK at T157 within the TDY motif and upregulates ICK kinase activity in vitro. The single (ADY and TDF) and double (ADF) T-loop mutants were generated in the mouse ICK sequence (positions 1 to 300). Wild-type as well as mutant constructs of GST-mICK(1–300) were expressed in *E. coli* and partially purified on glutathione-Sepharose beads. (A) Equal amounts of beads were subjected to either immunoblot (IB) analyses against anti-phosphoERK and anti-ICK(N) antibodies (top panel) or in vitro phosphorylationassay with MBP (bottom panel). (B) The bead samples from panel A were incubated with and without purified GST-Cak1p in the presence of [γ-^{32}P]ATP. The ^{32}P incorporation into the substrate GST-ICK(1–300) was shown in an autoradiograph (top panel), and the amount of substrate used in the assay was shown in an SDS gel (bottom panel). (C) A time course study on CAK phosphorylation for both *E. coli*-expressed ICK(1–300) and HEK293T-expressed ICK(1–300) was done essentially as for panel B. The amount of substrate used was indicated on SDS gels. (D) Analysis of the ICK phosphotransferase and MBP phosphotransferase activities of Cak1p-treated, *E. coli*-expressed ICK(1–300). Shown are ICK phosphorylation (top panel) and MBP phosphorylation (bottom panel) of *E. coli*-expressed GST-ICK(1–300) with and without Cak1p treatment. The amount of substrates used was indicated on SDS gels.

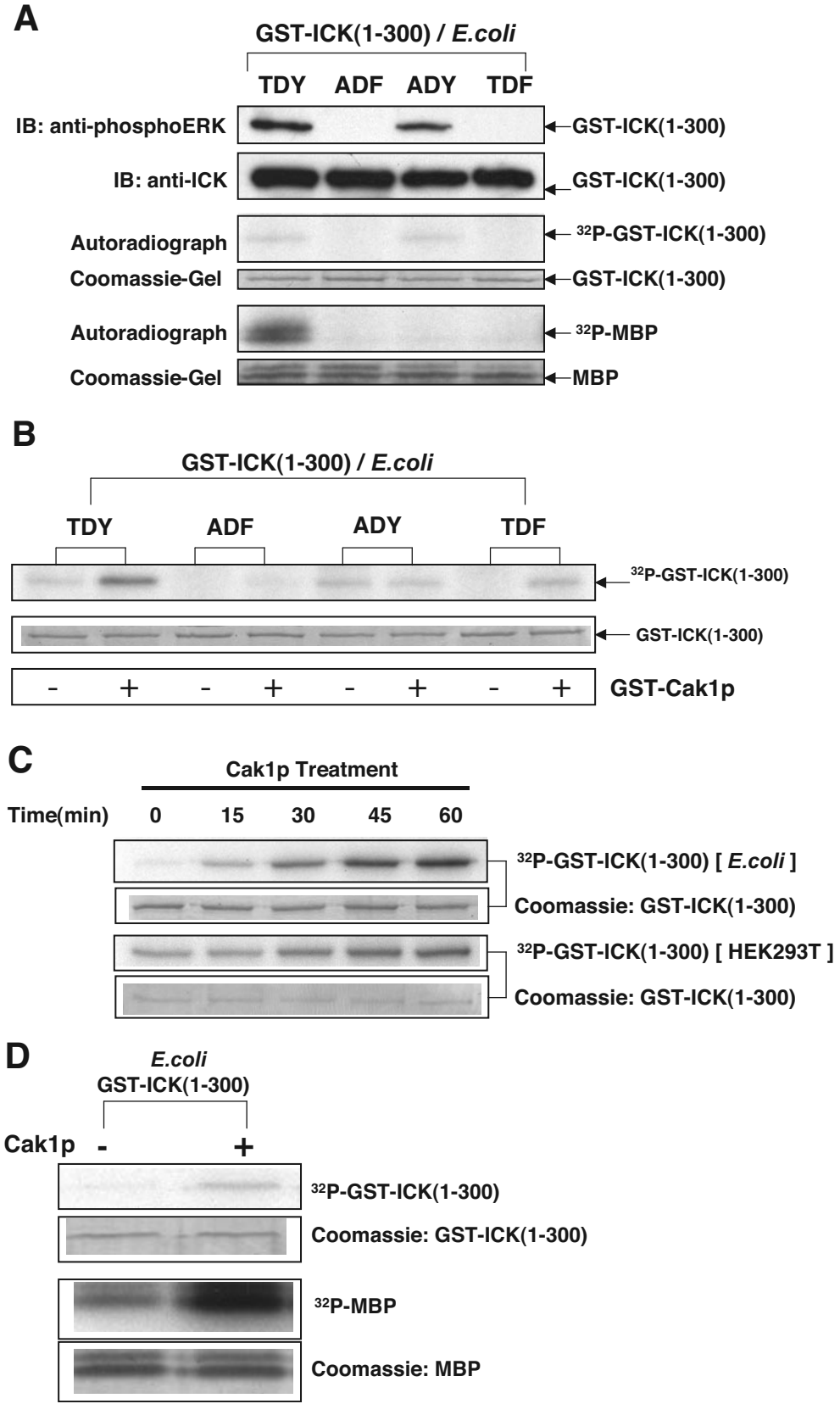
A
GST-ICK(1-300) / E.coli
TDY ADF ADY TDF
IB: anti-phosphoERK
GST-ICK(1-300)
IB: anti-ICK
GST-ICK(1-300)
Autoradiograph
32P-GST-ICK(1-300)
Coomassie-Gel
GST-ICK(1-300)
Autoradiograph
32P-MBP
Coomassie-Gel
MBP
B
GST-ICK(1-300) / E.coli
TDY ADF ADY TDF
32P-GST-ICK(1-300)
GST-ICK(1-300)
- + - + - + - +
GST-Cak1p
C
Cak1p Treatment
Time(min) 0 15 30 45 60
32P-GST-ICK(1-300) [E.coli]
Coomassie: GST-ICK(1-300)
32P-GST-ICK(1-300) [HEK293T]
Coomassie: GST-ICK(1-300)
D
E.coli
GST-ICK(1-300)
Cak1p - +
32P-GST-ICK(1-300)
Coomassie: GST-ICK(1-300)
32P-MBP
Coomassie: MBP

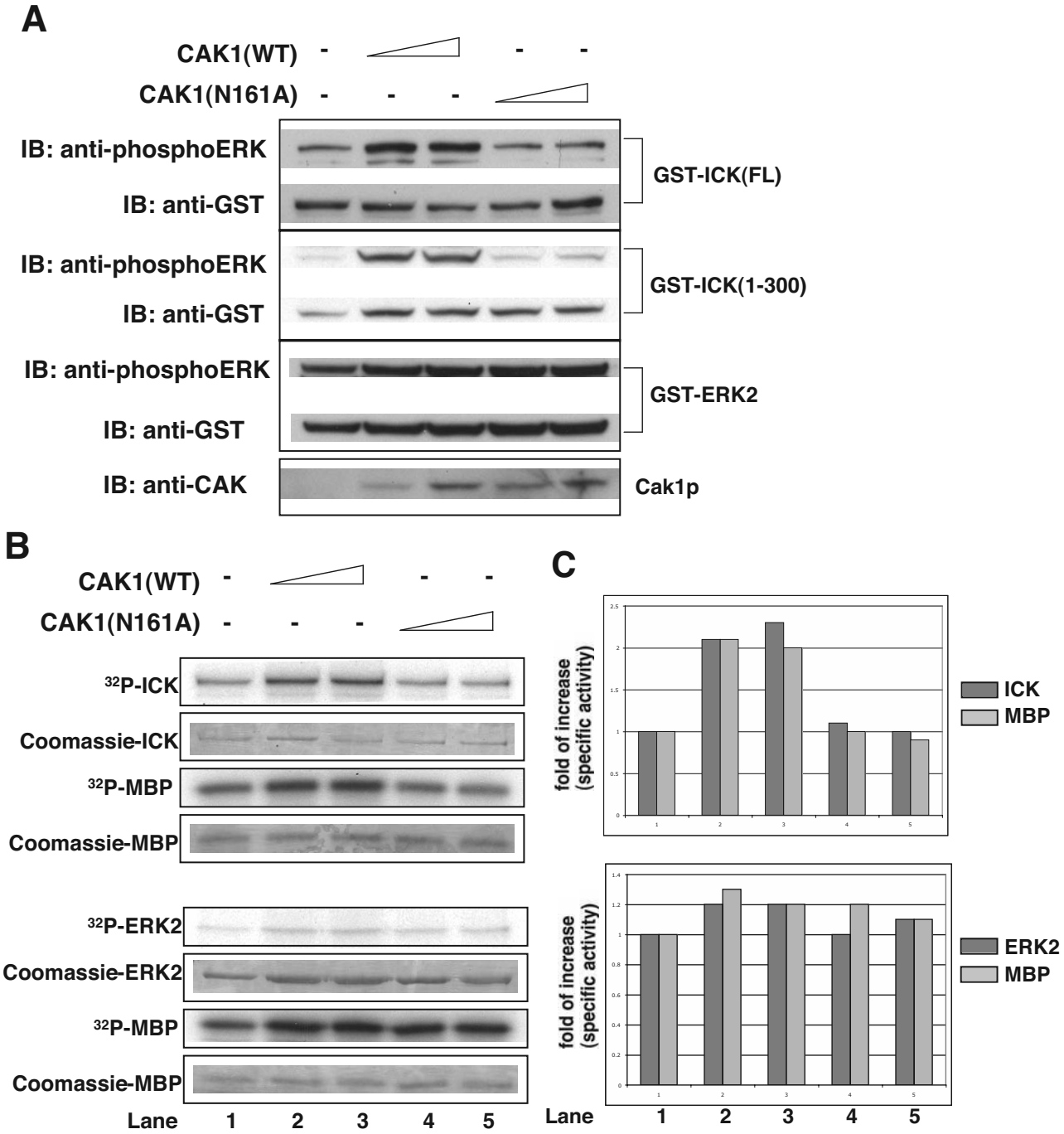

FIG. 10. CAK1 phosphorylates and activates ICK in cells. GST-ICK, GST-ICK(1–300), and GST-ERK2 (control) were cotransfected with either CAK1(WT) or kinase-inactive CAK1(N161A) in HEK293T cells. GST fusion proteins were pulled down with glutathione-Sepharose beads. The bead samples were subjected to either immunoblotting (IB) against the anti-phosphoERK and anti-GST antibodies (A) or in vitro kinase assay using myelin basic protein (B). Quantitation of ICK autokinase and MBP phosphotransferase activities from panel B is shown in panel C. Note that the reference for quantitation was the non-CAK1-expressed sample (lane 1). Results are representative of those from two independent experiments.

related to Ime2p. Apparent loop phosphorylation of Crk1 in the TEY motif is greatly reduced in a strain lacking Fuz7, a MAPKK, but whether Fuz7 could directly phosphorylate Crk1 was not determined (10a). These aspects remain to be explored.

Several pieces of our data can be rationalized if TDY motif phosphorylations are ordered, with tyrosine phosphorylation preceding threonine phosphorylation. By mass spectrometry, only the pTDpY and TDpY forms but not the pTDY form of ICK are detected in HEK293T cells. In addition, both in vitro and in vivo CAK1 phosphorylation data suggest that singly tyrosine-phosphorylated ICK is a preferred substrate for

CAK1. Since ICK can autophosphorylate on Y159, it appears that phosphorylation of Y159 serves to prime for T157 phosphorylation by CAK.

Studies of the role of phosphorylation of other TDY kinases will be required. It has been concluded that an ADF mutation of the TDY motif did not affect the basal or epidermal growth factor-stimulated phosphotransferase activities attributed to either CDKL1 (p42 KKIALRE) or CDKL2 (p56 KKIAMRE) (38). By contrast, activation of tagged NKIAMRE (CDKL3) in cells, by either phorbol ester or okadaic acid, is clearly abrogated in an ADF mutant (45). The reasons for the divergent results reported for CDKL3 versus CDKL1 and CDKL2 are unclear given their relatedness. MOK, like NKIAMRE, is activated by either phorbol ester or okadaic acid (24). An AEF mutant of MOK cannot be activated, and MOK is most similar to MAK and ICK in its kinase domain.

Our studies establish that only the catalytic domain of ICK is required for nuclear localization. Intact subdomain XI is required as well as the conserved arginine, R272. Neither kinase activity nor TDY phosphorylation appears to be necessary. Subdomain XI is part of a surface on the larger lobe of the core on the side opposite the catalytic cleft. This surface is not close to the substrate docking groove (lined by α_d and α_e and β_7-β_8) defined by a structure for p38 with MEF2A or MKK3 peptide (9) or by mutations (39). So far as we are aware, this is the first discovery of a possible role for subdomain XI in nuclear localization of a kinase. In DYRK1A, the preceding subdomains X and XI contain a structure sufficient for nuclear targeting (5).

Some characteristics of ICK resemble those of ERK7, and others do not. Both ICK and ERK7 are predominantly nuclear and require autokinase activity. Both ICK (data not shown) and ERK7 were not further activated by brief serum stimulation (3). Unlike the case for ERK7, the noncatalytic domain of ICK is not required for nuclear localization of ICK. ERK7 was reported to be dually phosphorylated on TEY when expressed in bacteria (2), but no mass spectrometry data were provided.

ICK's C-terminal domain has little or no similarity to the C termini of the large ERKs in primary sequence. However, each is proline-rich and is predicted to be highly charged and overall either very acidic or very basic: ICK, pI 10.06; MAK, pI 9.9; ERK7, pI 11.2; ERK8, pI 10.1; and ERK5, pI 4.84. The C-terminal domain of ERK5 has defined functions in nuclear localization, interaction with substrate MEF2, and transactivation (19). These different deductions suggest that the ICK COOH terminus may be a protein-nucleic acid or protein-protein interaction domain. We failed to identify any currently known motifs, folds, or domains within the C-terminal domain of ICK.

PROPSEARCH uses amino acid composition, and properties derived thereof, to generate vectors which can be used to search a vector database of proteins defining functional families (12). The best matches for human ICK(amino acids 265 to 632) returned from the human proteome are DNA binding proteins: pituitary homeobox 2, intestinal-enriched Krueppel-like factor, early response growth factor 3, paired box protein 8, brain-specific POU domain protein 4, hepatocyte nuclear factor 6, and HOX-3E (calculated PROPSEARCH reliabilities, 87 to 80%).

Nuclear localization of ICK suggests nuclear functions. ICK may regulate mRNA transcription or splicing. Given that MAK message is highly modulated in the meiotic cell cycle (23), MAK and ICK may have roles in the cell cycle. The most similar kinase to ICK in budding yeast is Ime2p, a gene induced in meiosis and required for sporulation. Mutations of the TXY motif in the T loop of Ime2p (Fig. 1B) cause loss of function (32), similar to the effect on ICK. Furthermore, Cak1p, the yeast homolog of CAK, has been shown to function early in meiosis to promote DNA synthesis through Ime2p (32), although the direct phosphorylation of purified Ime2p by purified Cak1p in vitro was not detected (31). In *Schizosaccharomyces pombe*, there are two candidate homologs of ICK, pit1 and mde3 (Fig. 1B). mde3 is induced in a meiotic transcriptional program (1), a possible parallel to MAK and Ime2p. Both ICK and Ime2p are most similar to pit1 in *S. pombe*. pit1 is expressed in cells that are growing and executing mitotic cycles and is not induced in meiosis (1). A *pit1*Δ *mde3*Δ strain has a more severe phenotype than a *mde3*Δ strain. The phenotype is an increased frequency of abnormal asci and nonsporulating spores.

ACKNOWLEDGMENTS

We thank Susan Taylor, Natalie Ahn, Steven Cohn, John Lawrence, Li-Zhi Mi, and Mike Hall for comments, encouragement, and/or advice, as well as members of the Sturgill laboratory (Carol Chrestensen, Gina Devasahayam, and Jacquelyn Kremper). Jacquelyn Kremper and Katherine Larson provided technical assistance, and Katrina Clines contributed to the cloning of ICK truncation mutants. We thank Bradford Berk, Bryce Paschal, Michael Weber, David Brautigan, and Mark Solomon for sharing reagents and constructs.

This work was supported by NIH grant GM62890 (to T.W.S.) and GM37537 (to D.F.H.) and by pilot funds from the Digestive Center for Health Excellence.

REFERENCES

1. **Abe, H., and C. Shimoda.** 2000. Autoregulated expression of Schizosaccharomyces pombe meiosis-specific transcription factor Mei4 and a genome-wide search for its target genes. Genetics **154:**1497–1508.
2. **Abe, M. K., K. T. Kahle, M. P. Saelzler, K. Orth, J. E. Dixon, and M. R. Rosner.** 2001. ERK7 is an autoactivated member of the MAPK family. J. Biol. Chem. **276:**21272–21279.
3. **Abe, M. K., W. L. Kuo, M. B. Hershenson, and M. R. Rosner.** 1999. Extracellular signal-regulated kinase 7 (ERK7), a novel ERK with a C-terminal domain that regulates its activity, its cellular localization, and cell growth. Mol. Cell. Biol. **19:**1301–1312.
4. **Abe, S., T. Yagi, S. Ishiyama, M. Hiroe, F. Marumo, and Y. Ikawa.** 1995. Molecular cloning of a novel serine/threonine kinase, MRK, possibly involved in cardiac development. Oncogene **11:**2187–2195.
5. **Alvarez, M., X. Estivill, and S. de la Luna.** 2003. DYRK1A accumulates in splicing speckles through a novel targeting signal and induces speckle disassembly. J. Cell Sci. **116:**3099–3107.
6. **Bladt, F., and C. Birchmeier.** 1993. Characterization and expression analysis of the murine rck gene: a protein kinase with a potential function in sensory cells. Differentiation **53:**115–122.
7. **Brown, N. R., M. E. Noble, A. M. Lawrie, M. C. Morris, P. Tunnah, G. Divita, L. N. Johnson, and J. A. Endicott.** 1999. Effects of phosphorylation of threonine 160 on cyclin-dependent kinase 2 structure and activity. J. Biol. Chem. **274:**8746–8756.
8. **Casanovas, O., F. Miro, J. M. Estanyol, E. Itarte, N. Agell, and O. Bachs.** 2000. Osmotic stress regulates the stability of cyclin D1 in a p38SAPK2-dependent manner. J. Biol. Chem. **275:**35091–35097.
9. **Chang, C. I., B. E. Xu, R. Akella, M. H. Cobb, and E. J. Goldsmith.** 2002. Crystal structures of MAP kinase p38 complexed to the docking sites on its nuclear substrate MEF2A and activator MKK3b. Mol. Cell **9:**1241–1249.
10. **Chrestensen, C. A., M. J. Schroeder, J. Shabanowitz, D. F. Hunt, J. W. Pelo, M. T. Worthington, and T. W. Sturgill.** 2004. MAPKAP kinase 2 phosphorylates tristetraprolin on in vivo sites including Ser178, a site required for 14-3-3 binding. J. Biol. Chem. **279:**10176–10184.

10a. **Garrido, E., U. Voss, P. Müller, S. Castillo-Lluva, and J. Pérez-Martín.** 2004. The induction of sexual development and virulence in the smut fungus *Ustilago Maydis* depends on Crk1, a novel MAPK protein. Genes Dev. **18:**3117–3130.

11. **Ge, B., H. Gram, F. Di Padova, B. Huang, L. New, R. J. Ulevitch, Y. Luo, and J. Han.** 2002. MAPKK-independent activation of p38alpha mediated by TAB1-dependent autophosphorylation of p38alpha. Science **295:**1291–1294.
12. **Hobohm, U., and C. Sander.** 1995. A sequence property approach to searching protein databases. J. Mol. Biol. **251:**390–399.
13. **Johnson, D. A., P. Akamine, E. Radzio-Andzelm, M. Madhusudan, and S. S. Taylor.** 2001. Dynamics of cAMP-dependent protein kinase. Chem. Rev. **101:**2243–2270.
14. **Kaldis, P.** 1999. The cdk-activating kinase (CAK): from yeast to mammals. Cell Mol. Life Sci. **55:**284–296.
15. **Kaldis, P., Z. W. Pitluk, I. A. Bany, D. A. Enke, M. Wagner, E. Winter, and M. J. Solomon.** 1998. Localization and regulation of the cdk-activating kinase (Cak1p) from budding yeast. J. Cell Sci. **111:**3585–3596.
16. **Kaldis, P., A. A. Russo, H. S. Chou, N. P. Pavletich, and M. J. Solomon.** 1998. Human and yeast cdk-activating kinases (CAKs) display distinct substrate specificities. Mol. Biol. Cell **9:**2545–2560.
17. **Kaldis, P., and M. J. Solomon.** 2000. Analysis of CAK activities from human cells. Eur. J. Biochem. **267:**4213–4221.
18. **Kaldis, P., A. Sutton, and M. J. Solomon.** 1996. The Cdk-activating kinase (CAK) from budding yeast. Cell **86:**553–564.
19. **Kasler, H. G., J. Victoria, O. Duramad, and A. Winoto.** 2000. ERK5 is a novel type of mitogen-activated protein kinase containing a transcriptional activation domain. Mol. Cell. Biol. **20:**8382–8389.
20. **Koji, T., A. Jinno, H. Matsushime, M. Shibuya, and P. K. Nakane.** 1992. In situ localization of male germ cell-associated kinase (mak) mRNA in adult mouse testis: specific expression in germ cells at stages around meiotic cell division. Cell. Biochem. Funct. **10:**273–279.
21. **Lavoie, J. N., G. L'Allemain, A. Brunet, R. Muller, and J. Pouyssegur.** 1996. Cyclin D1 expression is regulated positively by the p42/p44MAPK and negatively by the p38/HOGMAPK pathway. J. Biol. Chem. **271:**20608–20616.
22. **Liu, Y., C. Wu, and K. Galaktionov.** 2004. p42, a novel cyclin-dependent kinase-activating kinase in mammalian cells. J. Biol. Chem. **279:**4507–4514.
23. **Matsushime, H., A. Jinno, N. Takagi, and M. Shibuya.** 1990. A novel mammalian protein kinase gene (mak) is highly expressed in testicular germ cells at and after meiosis. Mol. Cell. Biol. **10:**2261–2268.
24. **Miyata, Y., M. Akashi, and E. Nishida.** 1999. Molecular cloning and characterization of a novel member of the MAP kinase superfamily. Genes Cells **4:**299–309.
25. **Miyata, Y., and E. Nishida.** 2004. CK2 controls multiple protein kinases by phosphorylating a kinase-targeting molecular chaperone, Cdc37. Mol. Cell. Biol. **24:**4065–4074.
26. **Murray, A. W.** 2004. Recycling the cell cycle: cyclins revisited. Cell **116:**221–234.
27. **Payne, D. M., A. J. Rossomando, P. Martino, A. K. Erickson, J. H. Her, J. Shabanowitz, D. F. Hunt, M. J. Weber, and T. W. Sturgill.** 1991. Identification of the regulatory phosphorylation sites in pp42/mitogen-activated protein kinase (MAP kinase). EMBO J. **10:**885–892.
28. **Richert, K., H. Schmidt, T. Gross, and F. Kaufer.** 2002. The deubiquitinating enzyme Ubp21p of fission yeast stabilizes a mutant form of protein kinase Prp4p. Mol. Genet. Genomics **267:**88–95.
29. **Rivard, N., M. J. Boucher, C. Asselin, and G. L'Allemain.** 1999. MAP kinase cascade is required for p27 downregulation and S phase entry in fibroblasts and epithelial cells. Am. J. Physiol **277:**C652–C664.
30. **Sancho, E., E. Batlle, and H. Clevers.** 2003. Live and let die in the intestinal epithelium. Curr. Opin. Cell Biol. **15:**763–770.
31. **Schaber, M., A. Lindgren, K. Schindler, D. Bungard, P. Kaldis, and E. Winter.** 2002. CAK1 promotes meiosis and spore formation in *Saccharomyces cerevisiae* in a CDC28-independent fashion. Mol. Cell. Biol. **22:**57–68.
32. **Schindler, K., K. R. Benjamin, A. Martin, A. Boglioli, I. Herskowitz, and E. Winter.** 2003. The Cdk-activating kinase Cak1p promotes meiotic S phase through Ime2p. Mol. Cell. Biol. **23:**8718–8728.
33. **Schroeder, M. J., J. Shabanowitz, J. C. Schwartz, D. F. Hunt, and J. J. Coon.** 2004. A neutral loss activation method for improved phosphopeptide sequence analysis by quadrupole ion trap mass spectrometry. Anal. Chem. **76:**3590–3598.
34. **Schultz, J., F. Milpetz, P. Bork, and C. P. Ponting.** 1998. SMART, a simple modular architecture research tool: identification of signaling domains. Proc. Natl. Acad. Sci. USA **95:**5857–5864.
35. **Schwede, T., J. Kopp, N. Guex, and M. C. Peitsch.** 2003. SWISS-MODEL: an automated protein homology-modeling server. Nucleic Acids Res. **31:**3381–3385.
36. **Shevchenko, A., M. Wilm, O. Vorm, and M. Mann.** 1996. Mass spectrometric sequencing of proteins silver-stained polyacrylamide gels. Anal. Chem. **68:**850–858.
37. **Shinkai, Y., H. Satoh, N. Takeda, M. Fukuda, E. Chiba, T. Kato, T. Kuramochi, and Y. Araki.** 2002. A testicular germ cell-associated serine-threonine kinase, MAK, is dispensable for sperm formation. Mol. Cell. Biol. **22:**3276–3280.
38. **Taglienti, C. A., M. Wysk, and R. J. Davis.** 1996. Molecular cloning of the epidermal growth factor-stimulated protein kinase p56 KKIAMRE. Oncogene **13:**2563–2574.
39. **Tanoue, T., R. Maeda, M. Adachi, and E. Nishida.** 2001. Identification of a docking groove on ERK and p38 MAP kinases that regulates the specificity of docking interactions. EMBO J. **20:**466–479.
40. **Togawa, K., Y. X. Yan, T. Inomoto, S. Slaugenhaupt, and A. K. Rustgi.** 2000. Intestinal cell kinase (ICK) localizes to the crypt region and requires a dual phosphorylation site found in map kinases. J. Cell Physiol. **183:**129–139.
41. **Wu, J., A. J. Rossomando, J. H. Her, R. Del Vecchio, M. J. Weber, and T. W. Sturgill.** 1991. Autophosphorylation in vitro of recombinant 42-kilodalton mitogen-activated protein kinase on tyrosine. Proc. Natl. Acad. Sci. USA **88:**9508–9512.
42. **Xia, L., D. Robinson, A. H. Ma, H. C. Chen, F. Wu, Y. Qiu, and H. J. Kung.** 2002. Identification of human male germ cell-associated kinase, a kinase transcriptionally activated by androgen in prostate cancer cells. J. Biol. Chem. **277:**35422–35433.
43. **Yan, C., H. Luo, J. D. Lee, J. Abe, and B. C. Berk.** 2001. Molecular cloning of mouse ERK5/BMK1 splice variants and characterization of ERK5 functional domains. J. Biol. Chem. **276:**10870–10878.
44. **Yang, T., Y. Jiang, and J. Chen.** 2002. The identification and subcellular localization of human MRK. Biomol Eng. **19:**1–4.
45. **Yee, K. W., S. J. Moore, M. Midmer, B. W. Zanke, F. Tong, D. Hedley, and M. D. Minden.** 2003. NKIAMRE, a novel conserved CDC2-related kinase with features of both mitogen-activated protein kinases and cyclin-dependent kinases. Biochem. Biophys. Res. Commun. **308:**784–792.